Evaluating parameter fitting and model design for unsaturated processes in peatlands

by

James Elliott

A thesis
presented to the University of Waterloo
in fulfillment of the
thesis requirement for the degree of
Master of Science
in
Geography (Water)

Waterloo, Ontario, Canada, 2019

AUTHOR'S DECLARATION

I hereby declare that I am the sole author of this thesis. This is a true copy of the thesis, including any required final revisions, as accepted by my examiners.

I understand that my thesis may be made electronically available to the public.

Abstract

Growing *Sphagnum* moss for peatland restoration and fibre farming requires the proper moisture regime be maintained; thus, there is a desire to optimize growth by creating ideal hydrological conditions. *Sphagnum* mosses have no roots, as such they rely on passive water migration through the pore network of the unsaturated zone created by the overlapping branches. Water supply and availability is dictated by the relationship between soil water content (θ), pressure (ψ) and hydraulic conductivity (K). Hydrological modeling of the unsaturated zone is a technique for evaluating different management strategies. However, it is uncertain which parameterization method is most suitable for field scale processes and which soil water retention model (approach) is the most acceptable to use. Parameterizations of the van Genuchten – Mualem (VGM) equation were done using RETC, curve fitting to steady state laboratory (SSL) experiments; and Hydrus-1D, inverse simulation to transient field (TF) experiments, with observations from steady state laboratory (SSL) and transient field (TF) experiments, respectively. The acceptability of each parameterization was tested by comparing soil moisture estimates based on forward simulations to observed soil moisture in two regenerated moss profiles, established in 1970 and 2006.

The TF model simulated soil moisture well, and had an RMSE of 0.05 and 0.06 for 1970 and 2006, respectively. The most error occurred during the wettest and driest periods of the simulation. Simulated soil moisture was consistently drier than the observed soil moisture, in the SSL simulation, and had markedly higher RMSE, 0.14 and 0.27 for the 1970 and 2006 profiles, respectively. The estimate of the VGM α parameter, an approximation of the inverse of the air-entry pressure, in the SSL parameterization was an order of magnitude higher than that of the TF parameterization. A sensitivity analysis revealed that α was the most sensitive parameter.

The TF parameterization method was more appropriate for characterizing the retention curve than the SSL method, as such, it was used to characterize different approaches: hysteresis and dual porosity. By using an approach that can represent hysteresis, model performance was improved during the wet and dry periods of the forward simulation (RMSE = 0.02). Using an approach that included hysteresis was only more successful when it was implemented with a scaling equation that prevented the pumping effect. The dual porosity approach (RMSE = 0.05) performed better than the VGM approach (RMSE 0.06) for the 2006 profile, but both approaches performed similarly for the 1970 profile (RMSE 0.05). The dual porosity approach may have been more effective in the 2006 profile because of the varied assemblage of moss species present, whereas the 1970 profile was a

monoculture. The parameters estimated in this study are appropriate for modeling managed or industrial peatlands where the water table is maintained near the surface; where the simulated soil moisture is expected to be within the calibrated range.

Acknowledgements

I would like to start by thanking my advisor, Dr. Jonathan Price, for giving a giving a planning student an opportunity to get their feet wet in a bog. His comments, criticism, and his example have encouraged me to be a better scientist.

Thanks to the UW Wetlands Hydrology lab for providing invaluable feedback, support, and insight on my trials and tribulations. Additonally, I would like to thank Dr. Maria Strack for here insight on statistics. Special thanks to Owen Sutton for helping me understand what first appear to be nebulous model parameters and indulging me with conversations on the philosophy of groundwater modeling. To my not friend Tasha-Leigh Gauthier, thanks for questioning and pushing me to become a better scientist and making endless hours in a windowless room a bit less endless.

Lastly, thanks to Jordan Blake for sticking it out with me, really really.

Table of Contents

List of Figures

List of Tables

Chapter 1
Introduction

Models are a collection of assumptions and mathematical representations of the natural environment. Although, they will never correctly represent reality, they have many useful applications (Konikow and Bredehoeft 1992). Within peatlands, soil moisture plays an integral part in water chemistry (Freeman and Reynolds 1993), gas exchange (McNeil and Waddington 2003), species diversity (Clymo 1973), plant stress (Hájek and Beckett 2008), and recovery from natural (Benscoter et al 2011) and anthropogenic disturbances (Price 1997). Within peatland research, unsaturated hydrology models have provided a method of evaluating various conditions moss may be subject to, such as different water table depths or atmospheric conditions (McCarter and Price 2014); or assess the feasibility of new management strategies, such as moss compression (Gauthier et al 2018). Furthermore, hydrological models have also been used to characterize unsaturated zone contaminant transport (Gharedaghloo et al 2018; Simhayov et al 2018), plant stress (Moore and Waddington 2015), and peatland function (Dixon et al 2017). Although models can be used to answer several questions, a single model will not be able to answer them all. An appropriately scoped model can be very instructive for answering single questions.

Recently, *Sphagnum* fibre farming is being considered as an alternative to restoring peatlands after they have been disturbed for peat harvesting (Brown et al 2017) or agriculture (Gaudig et al 2018). The objective of fibre farming is to maximize *Sphagnum* biomass accumulation by optimizing water availability, irrigation is being tested as a viable management strategy (Brown et al 2017; Gaudig et al 2018). The optimum water content for *Sphagnum* moss is available to maximize carbon uptake through photosynthesis (Silvola 1990; Flanagan 1996), but not restrict gas exchange (Silvola 1990). Furthermore, water table stability of the peatland is an important factor in moss photosynthesis and biomass production (Pouliot et al 2015; Brown et al 2017). Hydrological models are a useful tool for assessing the scalability of an operation, and how moss growth and species composition may change the water demand and irrigation strategies.

Peatland soils comprise living *Sphagnum* mosses growing overtop their decomposing remnants, where the porous media is composed of overlapping leaves and branches in varying states of decomposition (Hayward and Clymo 1982). Unsaturated processes, soil water retention and unsaturated hydraulic conductivity, are governed by the structure and connectivity of pores that dictate the relationship between soil moisture (θ), soil water pressure (ψ), and hydraulic conductivity

(*K*) (Vogel 2000). The structure of pores in moss is governed by moss type, and the level of decomposition (Hayward and Clymo 1982; Quinton et al 2009; McCarter and Price 2014; Moore et al 2015). The most commonly used approach to represent the relationship between θ, ψ, and *K*, in peatlands, is the van Genuchten – Mualem equation (Petrone et al 2008; McCarter and Price 2014; Moore and Waddington 2015; McCarter et al 2017; Gauthier et al 2018). It is a relatively simple system of equations that assumes a unimodal pore-size distribution; where the soil remains mostly saturated until air-entry, then it drains until it reaches a residual water content (Dettmann et al 2014). Additional processes can be represented by using a more complex approach, such as using an approach that assumes multi-modal pore-size distribution (e.g. Weber et al 2017a). Complex approaches can increase the flexibility of the model, which can reduce error; however, this is at the cost of unique parameters (Hopmans et al 2002). As such, increasing model complexity should be used only if it is beneficial to meeting the model objectives. Simulations of field conditions using the van Genucthen – Mualem (VGM) approach were unable to represent soil moisture in the wet and dry range of the retention curves and a more complex approach may be needed (Schwärzel et al 2006b; Schwärzel et al 2006a). Approaches that represent macropores as dual porosity (Dettmann et al 2014; Weber et al 2017a) and include hysteresis (Hayward and Clymo 1982; Naasz et al 2005) may be able overcome observed shortcomings of the VGM approach.

Parameterization of unsaturated process for organic soils has primarily been done through curve fitting, using data from steady state laboratory experiments, where the observation range varied greatly between studies (Weiss et al 1998; Moore et al 2015). Many authors have noted that obtaining complete and adequate datasets for the parameterization of unsaturated processes in organic soils is challenging due to their elastic nature (Weiss et al 1998; Schwärzel et al 2002; Quinton et al 2009; Wallor et al 2018). The alternative method to steady state parameterization is inverse estimation of transient laboratory or field experiments using a model that incorporates unsaturated flow processes (Schwärzel et al 2006a; Weber et al 2017a; Gharedaghloo and Price 2019). The inverse solution can be much more difficult to define because boundary conditions need to be defined in addition to an adequate range of pressure head, soil moisture, or flux observations (Carrera and Neuman 1986; Šimůnek and Hopmans 2002; Šimůnek et al 2009). Parameterization of a model that can accurately simulate soil moisture at the field scale is important in the management and operation of industrial peatlands for *Sphagnum* fibre farming.

The estimation of VGM parameters able to simulate soil moisture in *Sphagnum* moss at the field scale has received little attention. Furthermore, approaches that include additional processes,

such as dual porosity (Dettmann et al 2014; Weber et al 2017a; Weber et al 2017b) and hysteresis have been limited or non-existent. As such, the determination of adequate parameters and an appropriate approach can be used to further understand hydrological risk and management of natural and restored peatlands. The primary objective of this research is to assess the effectiveness of predicting soil moisture at the field scale in regenerated *Sphagnum* mosses using different parameterization techniques and soil water retention and conductivity models. The specific objectives are to:

a) Assess how parameters estimated from curve fitting of steady state retention experiments and inverse modeling of field observations can simulate field scale soil.
b) Assess which retention model most accurately describes field scale soil moisture dynamics.

1.1 General approach

This thesis is composed of two separate manuscript style chapters, which evaluate model parameterization and model selection for the purpose of simulating soil moisture dynamics at the field scale in regenerated moss. Field and Laboratory data were collected by Neil Taylor; I was primarily responsible for study design and parameterization, and writing the first draft of both manuscripts, and making modifications following feedback. The first manuscript (Chapter 2) compares two separate methods (steady state laboratory, transient field) for determining parameters to describe the soil water retention and conductivity curves of regenerated *Sphagnum* moss. Recommendations are made on which technique is best able to estimate a parameter set that can be used to simulate soil moisture dynamics at the field scale. The second manuscript (Chapter 3) evaluates which retention model is most suitable to simulate soil moisture in a regenerated *Sphagnum* moss profile. The parameterization method recommended in Chapter 2 was used in Chapter 3.

Chapter 2
Comparison of steady state and transient parameterization of unsaturated models

2.1 Introduction

Unsaturated zone hydrological process in peatlands have become a topic of increased interest over the past two decades because of their importance to horticultural applications (da Silva et al 1993), climate change resilience (Moore and Waddington 2015), restoration (McCarter and Price 2015), and carbon dynamics/plant growth (Strack and Price 2010). Unsaturated zone processes control the ability of a porous media to retain water and conduct water under negative pressure, which is dictated by the pore size distribution of the media (Mualem 1976; van Genuchten 1980). *Sphagnum* mosses are the dominant species in many peatlands, and the pore network is created by overlapping leaves and branches (Hayward and Clymo 1982). *Sphagnum* mosses are bryophytes that have no roots, which rely on water conveyed through the pore network under capillary forces. Thus, understanding unsaturated process is important to understand how peatlands develop, function, and persist. Hydrological models have been used as a tool to estimate unsaturated flow using the relationships between pressure (ψ), soil moisture (θ), and hydraulic conductivity (K). Typically, retention curves ($\theta(\psi)$) and hydraulic conductivity curves ($K(\psi)$) have been derived by fitting equations to laboratory observations (da Silva et al 1993; Gnatowski et al 2002; Price et al 2008). Fit parameters have usually been used to compare retention capacity of different functional groups (Gnatowski et al 2010; Moore et al 2015) or assess functional differences of mosses under synthetic conditions (McCarter and Price 2014; Gauthier et al 2018; Golubev and Whittington 2018). Very little work has been done to predict field scale soil moisture fitted parameters.

Early experiments captured the retention curve by using variants of the pressure cell method (da Silva et al 1993; Weiss et al 1998; Sherwood et al 2013; Hallema et al 2015). Briefly, the pressure cell method is conducted by placing a sample on a porous plate in a chamber and applying a positive pressure with a pump or hanging water column and measuring the outflow (da Silva et al 1993). The $K(\psi)$ relationship has simultaneously been discerned with pressure cells using transient instead of static outflow measurements (Gnatowski et al 2010). More recently, Price et al. (2008) and McCarter et al. (2017), which is a modification of Price et al. (2008), have developed a method to simultaneously determine the $\theta(\psi)$ and $K(\psi)$ relationships of mosses, whose structure is easily

deformable, using tension disks at both ends of the sample. Tension disks have been used to characterize soil-water properties at pressures ranging from ~-5 to ~-30 cm (Moore et al 2015); whereas pressure cells have been used gone bellow -15 000 cm (Weiss et al 1998).

In order to use soil water characteristic curves in models a function is fit to the θ(ψ) and K(ψ) observations. Curve fitting is the process in which parameters in a given equation are determined by fitting a function to empirical relationships using statistical techniques. When only retention data are being fit, the van Genuchten (VG) model is the most commonly used approach. Alternatives to the VG have been explored for peat soils, however in both cases the VG better fit the observations (Weiss et al 1998; Hallema et al 2015). An extension of the VG equation was done by Mualem (1976) to simultaneously fit both retention and hydraulic conductivity curves. The van Genuchten-Mualem equation (VGM) is the most widely used retention/conductivity equation within peatland literature (Price et al 2008; Price and Whittington 2010; McCarter and Price 2014; Moore and Waddington 2015; McCarter et al 2017; Gauthier et al 2018; Golubev and Whittington 2018). Its performance has been compared to the Brooks-Corey method with varying results, sometimes performing better (Londra 2010) or worse (Naasz et al 2005) . An alternative method to curve fitting is inverse simulation, which is the process of iteratively solving Richard's equation to best match transient observations of soil moisture and/or pressure head (Vrugt et al 2008). Inverse simulation has been done in laboratory (Gnatowski et al 2010; Weber et al 2017b; Weber et al 2017a; Gharedaghloo and Price 2019) and field studies (Schwärzel et al 2006a; Schwärzel et al 2006b). The VGM is a system of equations defined as:

$$S_e = \frac{1}{(1 + |\alpha\psi|^n)^m} \tag{1}$$

$$S_e = \frac{\theta - \theta_r}{\theta_s - \theta_r} \tag{2}$$

$$K(S_e) = K_s S_e^l \left(1 - \left(1 - S_e^{1/m}\right)^m\right)^2 \tag{3}$$

where S_e is the effective saturation, ψ is the pressure head [L], K_s is the saturated hydraulic conductivity [L T^{-1}], and θ, θ_r, and θ_s are the water content, residual water content, and saturated water content, respectively. The parameters α [L^{-1}], n, and l are fitting parameters that represent the

inverse of the approximate air-entry pressure, width of the pore size distribution, and the pore-connectivity, respectively. The parameter *m* is calculated as 1-1/*n*.

Although α is strictly a fitting parameter (Peters et al 2011), it approximates the inverse of the air entry pressure; larger values result in drainage occurring at pressures closer to zero. Moore et al. (2015) remarked that accurately defining α values is difficult because of the quick drainage in peat and decomposed *Sphagnum*. Trying to capture the pressure range at which air-entry occurs is extremely difficult for *Sphagnum* moss samples with the retention disk method because the samples drain before the experiment begins (Golubev 2018). An examination of different experimental methods for determining retention curves suggest that evaporation experiments are less impacted by premature drainage (Schelle et al 2013).

The combination of parameters *n* and *m* has been compared to the pore size distribution index from the Brooks and Corey equation (van Genuchten et al 1991). Similarly, Peters et al. (2011) has described *n* as the width of the pore size distribution when the restriction of *m* (1-1/*n*) is being employed. The description of *n* and other similar parameters as the width is not in reference to the range, but the shape of the pore-size distribution (Russo 1988; Kosugi et al 2002; Peters et al 2011; Zhang et al 2014; Weber et al 2017b; Wallor et al 2018). Larger values represent a narrower pore size distribution (large peak) and quicker drainage once the air-entry pressure has been exceeded (Peters et al 2011). The flexibility of the curve fitting process is reduced when *m* becomes fixed, however the likelihood of fitting unique parameters is increased (van Genuchten et al 1991). The parameter *n* will only fit to values below 1 when *m* is not fixed (Hallema et al 2015). Both Gnatowski et al. (2010) and Moore et al. (2015) have remarked that fixing the residual water content has the effect of decreasing *n*.

The parameter *l* is a fitting parameter that is related to pore-connectivity; effectively it controls how quickly the hydraulic conductivity decreases with pressure beyond air-entry (Mualem 1976). Within Mualem's hydraulic conductivity equation the hydraulic conductivity is reduced by the effective saturation. Values of *l* larger than 0 result in a quicker decrease, whereas those less than 0 results in a slower decrease in hydraulic conductivity. As such, values above 0 can be physically based on tortuosity measurements; however values less than 0 simply become another fitting parameter (Peters et al 2011; Ghanbarian et al 2013). Schaap and Leij (2000) suggest that *l* has no physical meaning and should only be used as a fitting parameter. For mineral soils, Mualem (1976) has suggested a value of 0.5; however further investigation has revealed a much larger parameter range (-16 to 2) (Wösten and Van Genuchten 1988). Although negative values are acceptable, Peters

(2011) remarks that there is a lower acceptable limit to l based on the values of α and n, where if exceeded the conductivity function will increase.

Due to the complex nature of the VG and VGM equations, non-linear least squares (nls) optimization has been used for curve fitting and inverse simulation. Up to 5 and 7 parameters may need to be fit for the VG and VGM models, respectively. To ensure adequate degrees of freedom, various parameters have been fixed (Schwärzel et al 2006b; McCarter and Price 2014), or removed all together (Weiss et al 1998). Several authors have noted the limitation that nls is a local solver and may converge on a parameter set that is incorrect (i.e. a local minima of the objective function); therefore, nls should be run several times with varying initial estimates to overcome this limitation (van Genuchten et al 1991; Šimůnek and Hopmans 2002; Schwärzel et al 2006a; Vrugt et al 2008; Šimůnek et al 2009; Gnatowski et al 2010; Šimůnek et al 2012). Global search methods provide an alternative fitting method, where values are randomly selected from a distribution to find the best combination that minimizes the error between the observed and simulated values; however, global search methods are more computationally intensive (Beven 1993; Vrugt et al 2008).

Parameter validation is the process in which a set of observations not used in parameter estimation are modelled to assess how well the parameters fit; however, it is seldom done for peat soils. da Silva et al (1993) and Weiss et al. (1998) validated parameters by direct measurements and cross validation of laboratory experiments, respectively. Although both studies presented a good fit during the validation they represented a simplistic version of field conditions; the media was homogenous and only subject to drainage. Schwärzel et al (2006a) conducted the first study to validate VGM parameters in peatlands using curve fitting, laboratory inverse simulation, and field inverse simulation. Price and Whittington (2010) validated parameters from a multi-step drainage experiment against separate drainage and evaporation scenarios and were found to fit very well. To date, validation has not been conducted with a wetting scenario.

Despite the large volume of work done to characterize unsaturated processes in the laboratory, virtually no attempts have been made to assess their validity in field conditions. Furthermore, several parameterization methods have been presented and the evidence suggests that there can be large discrepancies in their performance (Schwärzel et al 2006a; Schelle et al 2013; Moore and Waddington 2015). An improved understanding of unsaturated processes can be gained by assessing how different parameter fitting methods can simulate soil. Therefore, the main objective of this study is to determine the unsaturated parameters that accurately describe soil moisture dynamics in the field. Specifically, parameters derived from tension disk curve fitting and field inverse

simulation will be compared; and the ability of the parameters to simulate field soil moisture will be assessed using one dimensional hydraulic modelling.

2.2 Methods

2.2.1 Study site and sample preparation

Data for this study were originally collected and published by Taylor and Price (2015), for a full description of methods consult the original publication. The study site was a cutover peatland located south of Shippagan, New Brunswick (47°40′N, 64°43′W) and it is characterized by alternating raised baulks and lowered trenches as a result of traditional block-cut peat harvesting. Since abandonment in 1970, *Sphagnum* mosses spontaneously recolonized the trenches. Additionally, the site was selected for research in *Sphagnum* fibre farming. Beginning in 2004 plots of vegetation were removed and replanted with *Sphagnum* mosses every two years until 2010 (Landry and Rochefort 2009). Plot names indicate the year of abandonment (1970) or year of restoration. The profile at each plot was old cut-over peat overlain by moss layers of varying thickness reflecting the time since moss re-establishment (Taylor and Price 2015). To measure soil moisture, triplicate CS605 TDR probes were installed at depths of 2.5, 7.5, 12.5, and 17.5 cm; and 2.5, 7.5, and 12.5 cm for the 2006 and 1970-C plots, respectively. Soil moisture was measured hourly, with the exception of TDRs installed at 12.5 and 17.5 cm below the surface in the 2006 profile, which were manually measured several times a week (Taylor and Price 2015). Meteorological, soil moisture, and water table data were collected hourly at the 1970-C and 2006 plots. Although the 2010 plot was instrumented, the moss layer was not thick enough to be instrumented or adequately sampled, thus, it was not used in this study. Several experimental plots were established in regions with moss growth starting in 1970 (Taylor and Price 2015), since only the 1970-C plot was instrumented, it will be referred to as 1970 in this study. Samples of *Sphagnum* moss (n = 2 per profile) and cut-over peat (n = 1 per profile) were taken from the top 10 cm, the base of the moss profile and the cut-over peat of each plot; depths represent the midpoint of 5 cm samples. Soil water retention and unsaturated hydraulic conductivity were the determined in the laboratory (Taylor and Price 2015) using the modified tension disk method (McCarter and Price 2014; McCarter et al 2017). Following that, bulk density, porosity, and saturated hydraulic conductivity were measured (Taylor and Price 2015). The depth of samples and TDR probes will define the layers used in later model domains.

2.2.2 Determination of soil hydraulic parameters

The VGM parameters (α, n, l and m= 1-1/n) were determined in the RETC curve fitting software (van Genuchten et al 1991) based on the conductivity and retention data measured by Taylor and Price (2015) in steady state laboratory experiments for each layer, hereafter referred to SSL parameters. All measured water content and conductivity measurements at each pressure step were used for fitting unless there was clear evidence of measurement error. To assess for potential measurement error, the measured water content vs conductivity data were plotted on a log-log plot and fit with a linear trend line. Hydraulic conductivity decreases with water content due to less and smaller pathways. If the points trended horizontally or downwards for decreasing water content, they violated the assumptions of conservation of mass because hydraulic conductivity is maintained despite having smaller and fewer pathways. If points did not conform to these criteria it would suggest a measurement error and they were removed from curve fitting; approximately 7% of observations were removed. The residual water content (θ_r) was set as 0.05 for cut-over peat and moss layers below 15 cm, and 0.11 for all moss layers above 15 cm based on average values from Weber et al. (2017a). Measured values of total porosity (θ_s) and saturated hydraulic conductivity (K_s) were used (Taylor and Price 2015). All observations were weighted equally and hydraulic conductivity was log-transformed before fitting, to reduce the numerical difference between water content and hydraulic conductivity values caused by different units. RETC uses Marquardt's maximum neighbour method to minimize the weighted least squares objective function, which has the potential to get stuck in local minima based on the initial estimates of the fitted parameters (van Genuchten et al 1991; Šimůnek et al 2012). As such, initial estimates were manually changed to find an optimal fit based on a higher R^2, lower correlation between variables, smaller confidence intervals, and a lower objective function (Appendix B). Confidence intervals for SSL parameters were calculated be RETC during the curve fitting process.

Inverse simulation was done using Hydrus-1D v.4.16 to fit the soil hydraulic parameters (α, n, l and m= 1-1/n) to the observed field soil moisture data from Taylor and Price, (2015). Similar to RETC, Hydrus uses Marquardt's maximum neighbour method to minimize the weighted least squares objective function of the simulated and observed soil moisture (Šimůnek et al 2009). Confidence intervals were calculated by Hydrus during the inverse simulation. Inverse simulation was done on data from a transient field experiment and hereafter the parameters so derived will be referred to as TF parameters. Observation nodes were set at depths corresponding to TDR locations in the field. A 20 day subset was selected for the calibration period, starting at hour 800 of the observation period,

for the inverse simulation and uses the model domain as described below (Table 2-1). The calibration period was selected to encompass a large range of soil moisture. Initial estimates of the fitting parameters were those determined from SSL parameterization, the bounds of the parameters space were informed by literature values. The 1970 profile had no observation node in the peat layer; as such the inverse model parameters for the 2006 peat layer were used. Soil hydraulic parameters from the calibration period were then used to simulate soil moisture for the entire 82-day period.

Table 2-1: Soil moisture observation frequency during the calibration period

Profile	Layer	# of Observations
1970	1	480
1970	2	480
1970	3	480
2006	1	480
2006	2	446
2006	3	30

2.2.3 Model Setup

Hydrus-1D was used to numerically simulate soil moisture dynamics in the 2006 and 1970 plots for an 82-day period between May and August 2013, using the parameters estimated from SSL and TF methods. The model domains for both sets of parameters (SSL and TF) were identical to compare goodness of fit from each parameterization method. The model domains were 0.58 and 0.47 m tall and contained three and four layers for the 2006 and 1970 plots, respectively. Node spacing was 0.005 m (Figure 2-1). The thickness of the upper moss layers was each 5 cm, which corresponds to the size of the cores from the laboratory experiment and the observation range (thickness) of the TDR probes used in field. Layer three of the 1970 profile was 10 cm thick and covered the range of 10 to 20 cm below surface; it was parameterized with the 17.5 cm sample and the 12.5 cm TDR for the SSL and TF models, respectively (Figure 2-1). A variable pressure head from observed water table measurements was used to define the lower boundary condition. Observed precipitation and estimated potential evaporation from Taylor and Price (2015) were used to characterize the upper boundary condition. Potential evapotranspiration was calculated using the Priestley-Taylor method. The Priestley-Taylor alpha value was set to 1.26 as defined by Priestley and Taylor (1972) and previously used in peatlands by Petrone et al. (2008) and Price (1992). The soil water atmospheric vapour

equilibrium (*hCrita*) defines the pressure at which evaporation capacity is exceeded; evaporation is limited when pressure in the top node reaches *hCritA*, actual evaporation will be less than potential evaporation (Šimůnek et al 2009). Numerically, *hCritA* is used to increase model stability by specifying a lower pressure bound, which prevents pressure from changing dramatically based on small changes in water content near residual. A *hCritA* of -10 000 cm was used because it is the pressure that Thompson and Waddington (2008) and Goetz and Price (2015) suggest soil vapour equilibrium occurs. Initial soil moisture conditions were determined by TDR observations and water table depth at the first modelled timestep.

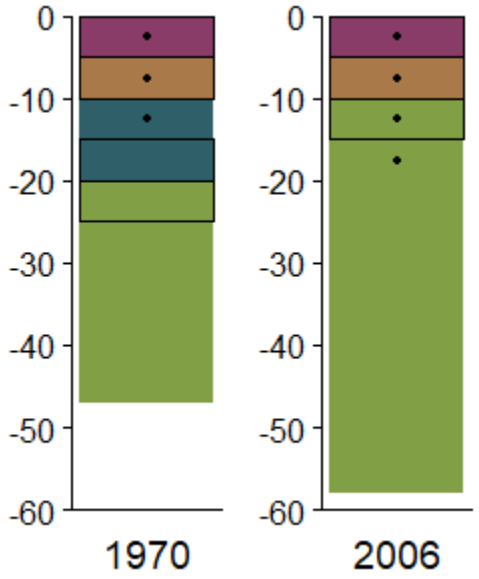

Figure 2-1: Model domain, TDR and sample depth

Model domain for the 1970 and 2006 profiles. The black dots are TDR/observation node depths, and black rectangles mark the location where samples were taken. The green layers are cut-over peat, and the remaining ones are regenerated moss.

2.2.4 Model performance

Model simulations of soil moisture for the 1970 and 2006 profiles were evaluated against observed observations for the 62 days of the 82-day observation period, excluding the calibration period, to assess the model performance using either RETC curve fitting and inverse simulation. Model performance was assessed using five statistical metrics: mean average error (MAE), root mean square

error (RMSE), mean bias error (ME), Nash-Sutcliffe efficiency (NSE), and modified Kling-Gupta efficiency (KGE'), such that:

$$MAE = \frac{1}{n'} * \sum |X_s - X_o| \tag{4}$$

$$RMSE = \sqrt{\frac{1}{n'} * \sum (X_s - X_o)^2} \tag{5}$$

$$ME = \frac{\sum X_s - X_o}{n'} \tag{6}$$

$$NSE = 1 - \frac{\sum (X_o - X_s)^2}{\sum (X_o - \overline{X_o})^2} \tag{7}$$

$$KGE' = 1 - \sqrt{\left(\frac{Cov_{so}}{\sigma_s * \sigma_o} - 1\right)^2 + \left(\frac{\sigma_s / \overline{X_s}}{\sigma_o / \overline{X_o}} - 1\right)^2 + \left(\frac{\overline{X_s}}{\overline{X_o}} - 1\right)^2} \tag{8}$$

where *n'* is the number of observed samples, and X, $\overline{X}$, and σ are the samples, means and standard deviations, respectively, for the corresponding subscript, simulated (*s*), and observed (*o*). Cov_{so} is the covariance between the simulated and the observed. The number of observation is denoted as *n'* to differentiate it from *n* in the VGM. MAE is a measure of average error magnitude, while RMSE is a more conservative quantification of error and is influenced more by larger errors. ME indicates whether the simulations tends to over (positive) or under (negative) predict the observations and is expressed as in original units. The NSE is a measures of overall model performance that compares the performance of the simulation to the performance of the mean (Nash and Sutcliffe 1970). KGE' is a multi-objective approach that combines correlation, simulated-observed mean ratio, and variability (Kling et al 2012). Ideal values of NSE and KGE' are unity and have no lower limit; values above 0.7 were considered an acceptable fit. All error metrics were computed in R 3.5.0 (R Core Team 2018) with the hydroGOF package (Mauricio Zambrano-Bigiarini 2017).

The observed soil moisture was plotted against simulated soil moisture for each profile and fitting method. Linear regressions and t-tests of the regression coefficients were performed to see if the regression lines were significantly different from the 1:1 line (Paternoster et al 1998). A

statistically significant slope or intercept from 1 and 0 indicate that the simulation is inconsistent with the observations, or that the model is biased, respectively (Mesplé et al 1996; Piñeiro et al 2008). All statistical analysis excluded the calibration period, simulation time 800 to 1280 h, to ensure only the validation period is being assessed.

A sensitivity analysis was done to assess which parameters had the greatest impact on model accuracy by individually increasing and decreasing α, n, and l by 10 steps, incremented by $log(0.15)$, 0.03, and 0.5, respectively. Intervals were selected to represent a large portion of the parameter space presented by literature values (Figure A-1:A-3). The sensitivity analysis was done on both profiles and fitting methods, and all fitted layers. The TF parameterization was repeated with an alternate set of initial estimates (ALT) to assess how final parameter estimates would change and the impact it would have on the overall model fit. The alternate estimates came from the average value of their equivalent depth form (Weber et al 2017b). There was no cut-over peat, as such initial estimates of the 1970 and 2006 peat layers were from the 37.5 cm layer.

2.3 Results

2.3.1 Parameter fitting

The SSL fitting method produced curves that agreed well with the laboratory observations. All curves had an R^2 above 0.8 with the exception of the 1970 – 17.5 layer, which had an R^2 of 0.73. The drainage of the moss layers was immediate and relatively quick but was delayed and more gradual for the peat layers (Figure 2-2). The 2.5 and 7.5 cm retention curves from TF model showed that drainage would start at a higher pressure than the SSL curves. Similarly, the lowest TF layers (1970 – 17.5 and 2006 – 12.5) started to drain at a lower pressure and drained substantially quicker than their SSL counterpart (Figure 2-2). The trends in hydraulic conductivity curves were the same as those in the retention curves (Figure 2-3).

The estimates of the VGM parameters for the 1970 and 2006 SSL and TF profiles differed (Table 2-2) despite both RETC and Hydrus reporting a good fit during curve fitting and inverse simulation, respectively. The parameter α decreased with depth for both parameter estimation methods and profiles (Table 2-3). Additionally, the TF method yielded α values that had smaller confidence intervals, as such they were well defined. SSL values of n were higher in moss layers than cut-over peat, whereas those from TF modelling were the opposite. The 1970 and 2006 SSL, and 2006 TF profiles had l values that increased with depth; no trends were present in the 1970 TF profile.

The 2006 and 1970 SSL peat layers and 1970 TF 17.5 layer all had very large *l* values. Based on the confidence intervals, parameter *n* was generally well defined for all fitting methods, whereas *l* values fit with the TF method, or lower layers fit with SSL were poorly defined. An exception to the trends presented for the confidence intervals of α and *n* was the 2006 TF peat layer; both of which poorly defined.

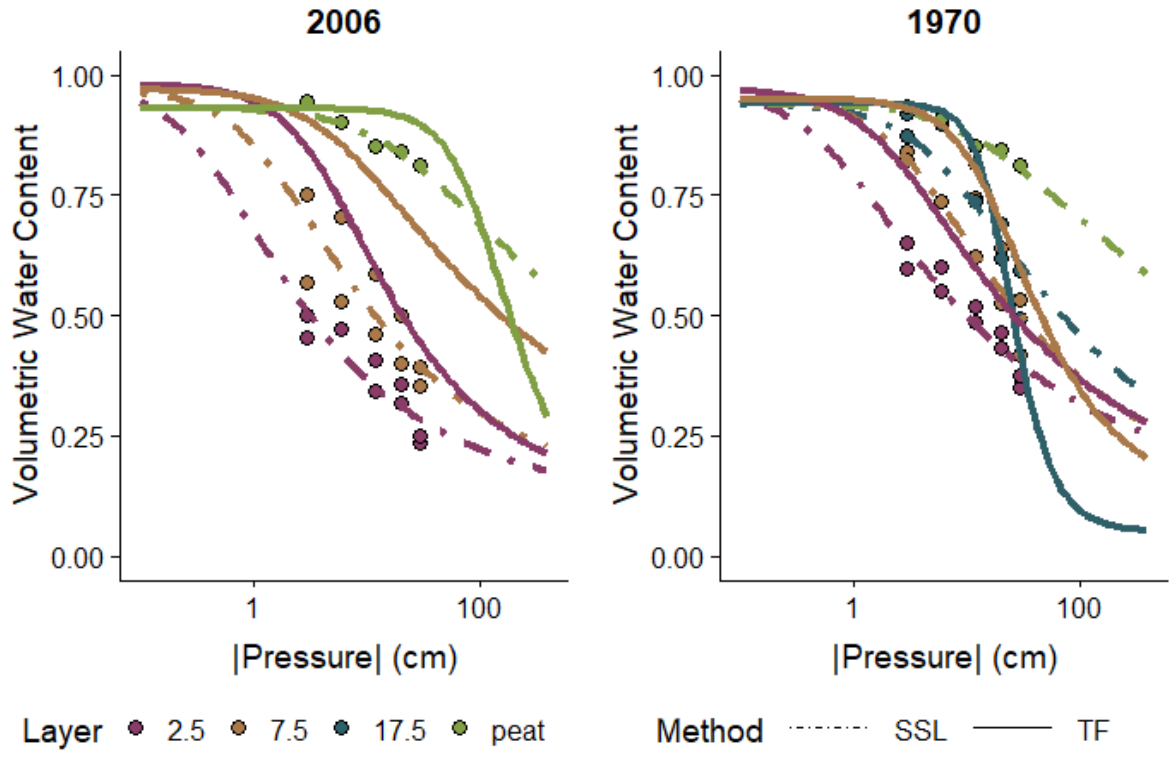

Figure 2-2: SSL and TF soil moisture retention curves

Retention curves for each profile fit to the laboratory observations (points) and the field observations.

2.3.2 Model Performance

Figure 2-4 depicts simulated and observed soil moisture over the modelled period for the 1970 and 2006 profiles fit with both methods. Visually, the TF fit better than the SSL model, with the poorest fit in the top two layers of each profile. Notably, the peat layer of the 2006 SSL model started to desaturate, yet it did not in the TF simulation. The TF simulations visually matched the observed

much better; however, both profiles underestimate soil moisture during the initial period with large soil moisture fluctuations and overestimate during the driest period.

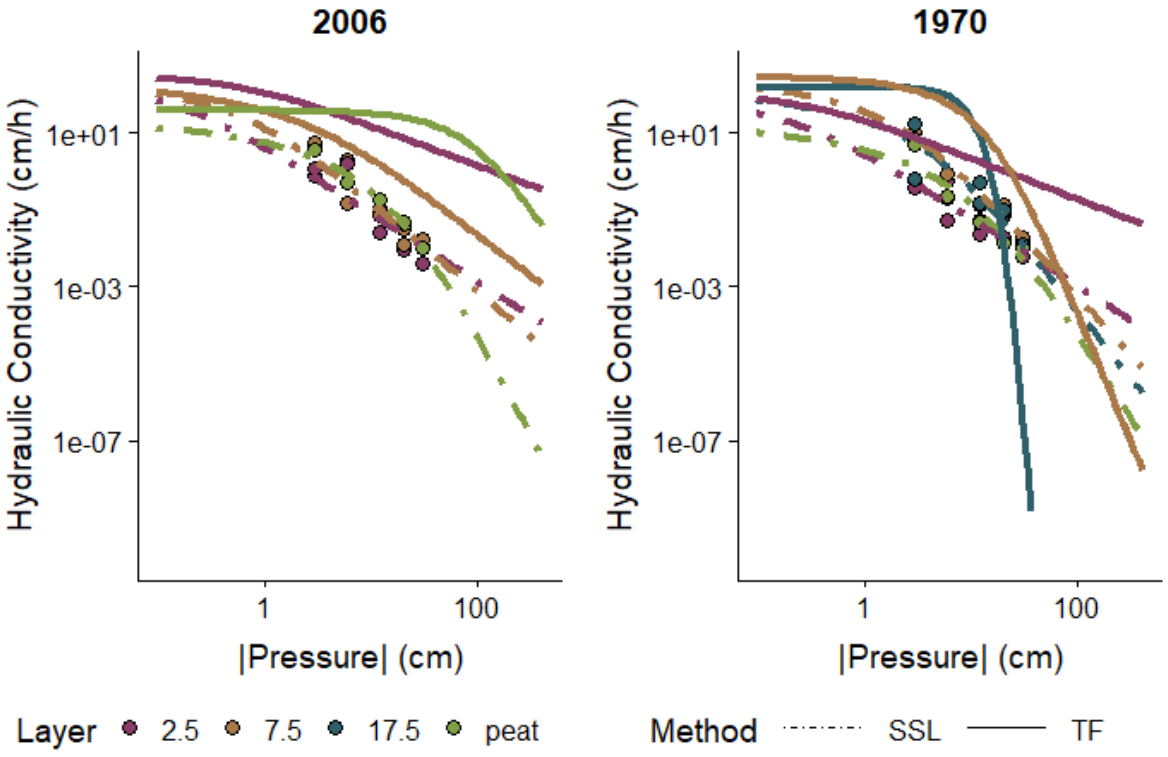

Figure 2-3: SSL and TF hydraulic conductivity curves

Retention curves for each profile fit to the laboratory observations (points) and the field observations.

Within each model, the RMSE and MAE were similar; as such most errors had a similar magnitude and RMSE was used to compare model performance (Table 2-3). As previously reported, the SSL curve fitting parameters resulted in a model that fit poorly where the RMSE of the 1970 and 2006 plots were greater than their respective TF plots by 0.09 and 0.21. The RMSE of the TF models were at the threshold of probe error, ~0.05. SSL models had negative ME, whereas the ME of TF models was approximately 0. The poor performance of the SSL profiles is reflected in low NSE and KGE', although both metrics were below 0.7 the KGE' is notably higher than the NSE. Conversely the NSE and KGE' scores for the TF models were both above 0.7. The mass balance error calculated by Hydrus was less than 1% for all simulations.

The linear regression of the observed and simulated soil moisture for the SSL profiles had slopes and intercepts that were statistically different ($p << 0.05$) from one and zero, respectively, suggesting that the model did not fit well (Figure 2-5). Similarly, the slope and intercept of TF model were also statistically different ($p << 0.05$), despite the good fit indicated by the error metrics; suggesting that the model may not represent all pertinent processes. However, the extremely small p-values may be a result of the large sample size (Sullivan and Feinn 2012).

Table 2-2: Model parameters and the 95% confidence interval

Method	Plot	Depth	α (cm^{-1})	α CI	*n*	*n* CI	*l*	*l* CI
TF	1970	2.5	0.47	0.04	1.31	0.01	-5	5.92
TF	1970	7.5	0.06	0	1.69	0.05	5	51.56
TF	1970	17.5	0.05	0	2.87	0.23	18.38	84.87
TF	2006	2.5	0.26	0.02	1.46	0.02	-4.11	49.92
TF	2006	7.5	0.18	0.02	1.23	0.02	-1.46	11.09
TF	2006	peat	.93	0.05	1.96	7.84	0.16	141.79
SSL	1970	2.5	1.71	0.91	1.28	0.05	-2.85	1.7
SSL	1970	7.5	0.3	0.12	1.34	0.08	1.1	2
SSL	1970	17.5	0.18	0.11	1.27	0.11	3.87	5.45
SSL	1970	peat	0.08	0.04	1.15	0.06	14.7	15.1
SSL	2006	2.5	2.7	2.2	1.37	0.1	-2.61	1.7
SSL	2006	7.5	0.81	0.6	1.34	0.12	-1.08	2.57
SSL	2006	peat	0.05	0.01	1.17	0.04	17.92	8.38
ALT	1970	2.5	0.28	0.06	1.57	0.08	1.18	1.49
ALT	1970	7.5	0.17	0.04	1.41	0.09	0.03	35.03
ALT	1970	17.5	0.08	0.02	1.52	0.26	2.53	141.67
ALT	2006	2.5	0.26	0.04	1.55	0.06	1.16	1.36
ALT	2006	7.5	0.16	0.03	1.38	0.05	0.01	15.25
ALT	2006	peat	0.01	0.03	1.21	2.03	1.87	2774.77

The forward simulation for both profiles and fitting methods were most sensitive to changes in α and least sensitive to l (Figure 2-8). Adjusting α parameters of the upper layers in the SSL models and the 1970 TF model reduced the RMSE by up to 0.01 and 0.075 from the original parameterization. Changes in the parameter l increased or decreased the RMSE of the TF forward simulation by less than 0.01. The SSL forward simulation was more sensitive to changes in l than the TF model; the RMSE decrease by 0.02 and increase by 0.04 from 0.14 and 0.27 for the 1970 and 2006 profiles, respectively.

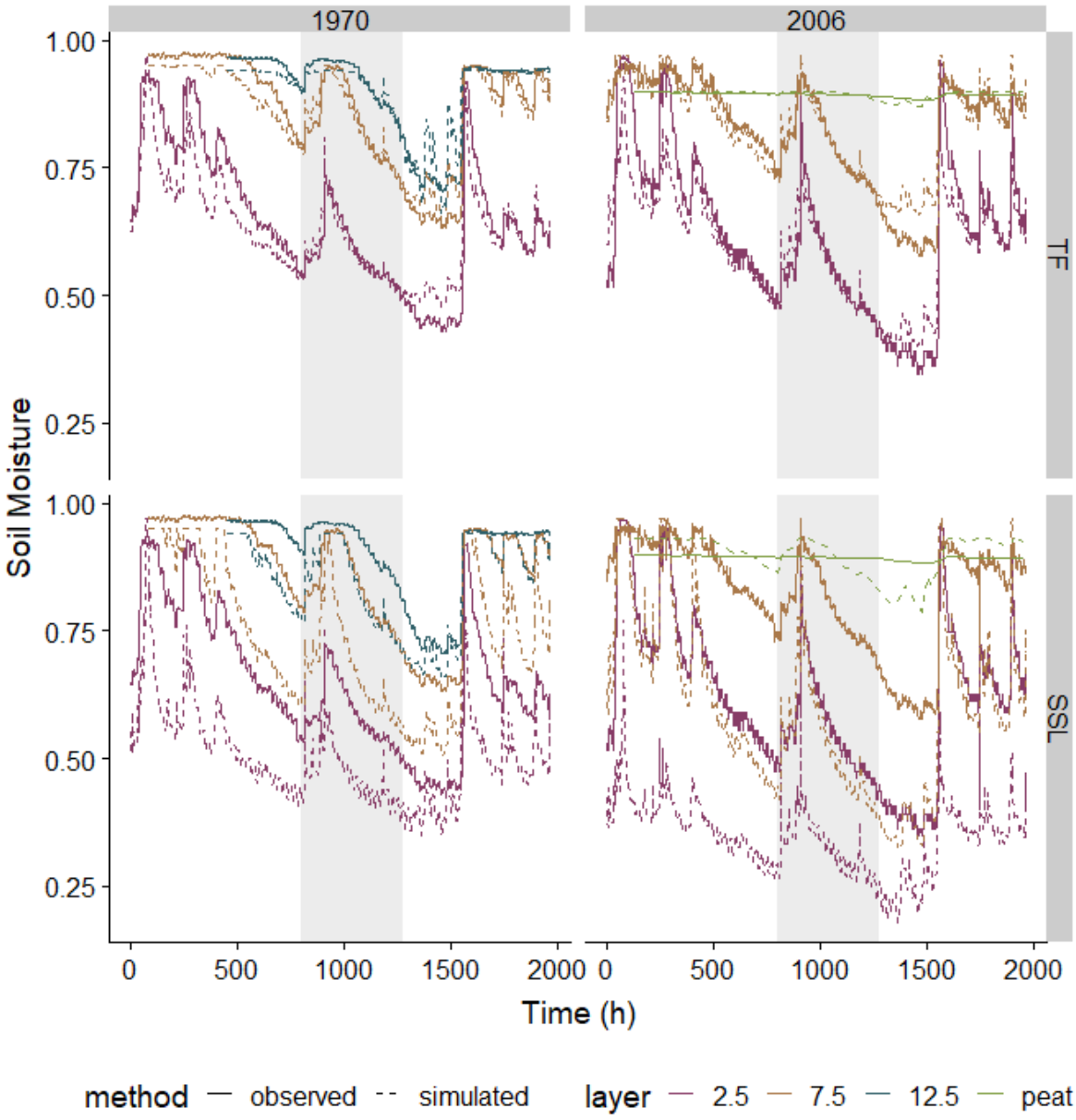

Figure 2-4: SSL and TS forward simulation of soil moisture

Time series of observed and simulated soil moisture for all models. The shaded grey area denotes the calibration period. Both observed and simulated nodes in the peat layer behaved the same; the lower one (17.5 cm depth) was removed for simplicity.

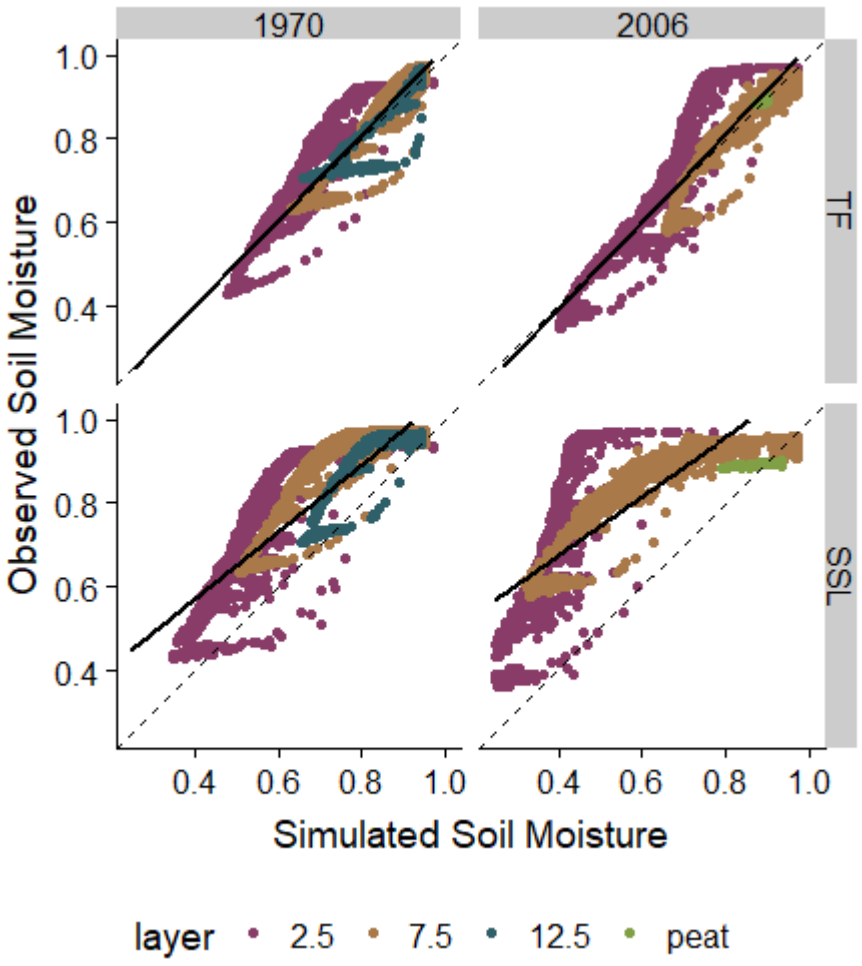

Figure 2-5: Regression of simulated and observed soil moisture

Regression of observed and simulated soil moisture. The solid line is the regression of the observed and simulated soil moisture and the dashed line is the hypothetical 1:1 relationship.

2.4 Discussion

2.4.1 The influence of fitting method on parameters

Based on model performance, parameters fitted using empirical curves from laboratory experiments (SSL) were not able to simulate soil moisture dynamics in the field, despite good agreement with

laboratory curves. The majority of observed soil moisture values in all moss layers occurred above the highest moisture measurement used for SSL fitting in RETC (Figure 2-6). It is possible that the laboratory parameters are unable to represent field conditions because of hysteretic effects on soil moisture when preparing the sample for the experiment (Golubev 2018). A laboratory sample may drain beyond the first pressure step such that the soil moisture is no longer on the main drying curve for the first pressure step, but between the main drying and wetting curve, on a scanning curve. A similar discrepancy was proposed by Schelle et al (2013) when comparing retention curves from evaporation experiments and suction plates in sandy soils. When laboratory observations of the θ-ψ curve are overlain on the estimated θ-ψ curve from the field, generally laboratory observations align with the wetting/scanning curves of the estimated field retention curve (Figure 2-6). This suggests that the retention disk method captured a scanning curve far removed from the main drying curve. It is possible that as the samples were removed from their saturated condition and set onto the tension disks, they drained beyond several pressure steps. As such, retention values may represent a scanning curve rather than the main drying curve. It would not be unreasonable to assume similar limitations using pressure cells (Moore et al 2015). Although pressure in the field was not measured, it can be deduced from the water table level as a linear 1:1 decrease with height above the water table (Lindholm and Markkula 1984), assuming drainage to the equilibrium condition, which does not occur under transient atmospheric conditions (Thompson and Waddington 2008). Equilibrium is likely for our study because the observation period was wetter than the 30 year average (Taylor and Price 2015). However, if the assumption of equilibrium is violated and evaporation has decreased pressure further than the 1:1 relationship, drier field observations would be associated with lower pressures, further deviating from laboratory observations. Alternatively, the samples taken may not be representative of field conditions due to the small sample size. However, other studies that parameterized α using data from the original and modified retention disk experiment (Price et al 2008; Price and Whittington 2010; McCarter and Price 2015; Gauthier et al 2018; Golubev and Whittington 2018) had values similar to this study.

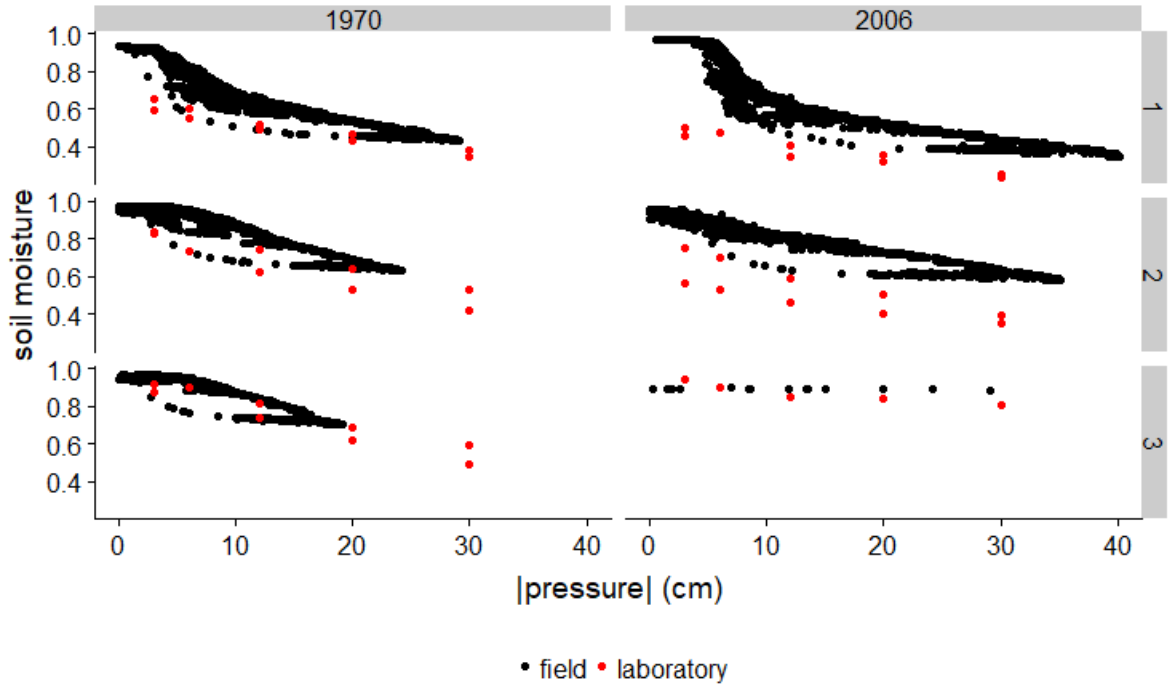

Figure 2-6: Observed SSL and assumed TF θ-ψ relationships

Superposition of laboratory retention curves on field retention curves for each layer. Pressure of the field observations is assumed from the depth of the water table below the soil moisture observation point. Layer 3 of the 2006 prole has less observed field because soil moisture was recorded manually and not logged.

Table 2-3: Model error statistics

Method	Plot	MAE	ME	RMSE	NSE	KGE'	Pearson r
SSL	2006	0.25	-0.25	0.27	-1.4	0.23	0.82
SSL	1970	0.12	-0.11	0.14	0.24	0.63	0.9
TF	2006	0.04	-0.01	0.06	0.89	0.89	0.95
TF	1970	0.04	-0.02	0.05	0.91	0.93	0.96
ALT	2006	0.04	0	0.06	0.89	0.83	0.95
ALT	1970	0.06	-0.01	0.07	0.79	0.77	0.9

The α parameter consistently decreased with depth for both fitting methods and profiles, which matches virtually all literature trends (Figure A-1; Moore et al., 2015). Decomposition and compression decreases the number of large pores and increase bulk density, which has been found to be inversely related to α; As such, a smaller value is expected with depth, especially in the older cut over peat, because it is highly decomposed and much denser (Bloemen 1983; Weiss et al 1998; Sherwood et al 2013; Moore et al 2015). Additionally, the α parameter was greatly impacted by the parameterization. The α values from SSL were higher than those from TF because SSL soil moisture observations were less than those of TF at equivalent pressure (Figure 2-6); however, they were well within the range of literature values (Figure A-1). This is due largely to the difference in water content at equivalent pressure in the data used for parameterization between the two methods (Figure 2-6). If other steady state experiments reported in the literature were also subject to large drainage after saturation and before the experiment began, α may be overestimated because the curve was fit to observations akin to a scanning curve rather than the main drying curve. Although not unreasonable estimations, the SSL α values had large confidence intervals (Table 2-2). Conversely, the moisture content during the TF calibration period included saturation for all layers with the exception of 1970 – 2.5, which would suggest that α should be more reliable. The confidence intervals for all TF layers were very small, supporting a better fit. The 2006 TF peat layer (12.5 cm layer) was the exception; this is most likely due to the extremely narrow range of soil moisture that it experienced. The water table was on average 14 and 17 cm below the surface with a standard deviation of 6.7 and 8.9 cm for the 1970 and 2006 plots, respectively. As such the large MAE for SSL models is most likely due to drainage occurring close to zero pressure. The superior fit to TF experiments for the parameter α was further demonstrated during rain events (Figure 2-4). The soil moisture is generally maintained after an event and matches the observed drying whereas the SSL model desaturates immediately after precipitation stops (Figure 2-4). Model fit has been found to be sensitive to α in this study (Figure 2-8) and others (Weiss et al 1998; Kettridge et al 2016); as such accurate characterization is important.

Unlike α, the parameter n was very well defined for the SSL models (Figure 2-8); this is most likely due to the majority of the laboratory observations being within the moisture range where drainage occurs. Assuming that the SSL experiment captured a scanning curve, rather than the main drying curve, there is reason to believe that the parameter n should still be reasonably accurate. Implementations of models that include hysteresis assume that n is equal for the wetting and drying branch of the retention curve (Šimůnek et al 2009). Thus, it is reasonable to extend the assumption to include scanning curves. The appropriate rate of drainage is reflected in the high R^2 for the RETC

models; 0.9 and 0.82 for 1970 and 2006, respectively. Literature values for *n* from curve fitting and inverse simulation generally decreased with depth; values from both SSL profiles were consistent with the trends (Figure A-1). Despite the TF model fitting well, having higher correlation, and values within range of the literature, it produced *n* values that were inconsistent with depth, likely due to an insufficient soil moisture range during calibration. Retention curves for lower layers (1970 – 17.5 cm and 2006 – peat) suggest the peat drains quickly once air-entry occurs (Figure 2-2). In general, large pores become compressed and fill with decomposing organic matter with depth, and the pores responsible for air entry drain at more negative pressures (smaller α). Furthermore, the width of the pore size distribution also increases (lower *n*) with depth. Similar to α, *n* has been shown to be inversely related to bulk density (Weiss et al 1998; Sherwood et al 2013; Moore et al 2015). This suggests that the *n* values from the bottom layers of the TF models are too large and not realistic because it is increasing with bulk density. In other studies, it has been found that fitting the residual water content, instead of fixing it like in this study, will result in higher estimates of *n*, which are inversely related to bulk density (Naasz et al 2005; Gnatowski et al 2010; Londra 2010; Dettmann et al 2014; Moore et al 2015; Weber et al 2017b). Price et al (2008) report *n* values higher than virtually all studies using a fixed residual water content, this discrepancy may be due to the weighting factor applied to the hydraulic conductivity data during curve fitting.

The forward simulations were not sensitive to changes in *l*, especially lower layers, and were generally poorly defined (Figure 2-8). In particular, SSL estimates for 1970 and 2006 peat layers were far beyond what has previously been reported in the literature (-5 to 5; Figure A-1). Although it is sensible to think that deeper more decomposed layers should have a higher *l* (Gnatowski et al 2010; Rezanezhad et al 2010; Gharedaghloo et al 2018), the magnitude of the SSL and TF 1970 – 17.5 layer and the peat layers in both profiles seems unreasonably high. It is likely that the range of measurements does not contain the required information to accurately predict *l.* Additionally, the majority of literature values from empirical curve fitting were all negative (Figure A-3), notably foundational work done by Price et al (2008) and McCarter and Price (2014a). The exceptions were Londra (2010) and McCarter et al. (2017), which were repacked horticultural peat, and the cutover peat sample from Gauthier et al (2018). Furthermore, *l* generally increased with depth, which suggests that it is related to bulk density and the level of decomposition. The *l* values from TF estimations were substantially different from SSL estimations, with the exception of the 2006 moss layers. Despite the difference in *l* between fitting methods, it is not likely to be responsible for the difference in model fit based on the large confidence intervals and the sensitivity analysis (Figure 2-8). Fixing *l*

at a constant value would reduce the complexity of the problem, in doing so at a physically meaningful value would be logical. To date Weber et al (2017a) are the only ones to report *l* values that can almost all be considered physically true (mean 1.36, SD 0.74 for VGM1) based on the definition provided by Peters et al (2011). Gharedaghloo et al (2018) reported tortuosity values from modelling experiment of ~2, which were higher than those estimated by Weber et al (2017a). Fixing *l* at ~2 during parameter inverse simulation resulted in estimates of α and *n* that were virtually identical to when *l* was free to vary (data not shown), which is reasonable because *l* was not a sensitive parameter in the forward simulation (Figure 2-8). Dettmann et al. (2014) suggests that *l* has little effect on soil moisture dynamics in peat and *Sphagnum* when pressure is above -200 cm. The pressure range experienced during the calibration period was greater than the -200 cm threshold, which supports the idea that inadequate information was available. As such, *l* should simply be considered a fitting parameter, regardless if it is positive or negative.

2.4.2 Did the model actually fit?

The parameters from SSL method were not able to simulate the observed soil moisture well at any depth when validated with field soil moisture measurements (Figure 2-4). The RMSE was several times larger than the TF models (Table 2-3). The RMSE, MAE, and ME of each SSL profile are approximately the same within each profile, which suggests that the entire fit was consistently poorly predicting soil moisture in the same manner. As in the study by Schwärzel et al (2006a), the SSL profiles under predict soil moisture, which is most likely a consequence of the high α parameter values. Moore et al. (2015) hypothesized that α cannot be accurately characterized in retention experiments if the first pressure step is below -100 cm. This cautionary note should be extended to all steady state laboratory experiments (tension disk and pressure cell) because drainage can occur before the sample is in the apparatus (Golubev 2018), and estimates of α similar between both types of experiments (Figure A-1). The models were very sensitive to α, as such it is important to accurately characterize the initial drainage. Weiss et al (1998) also found α to be a sensitive parameter and recommended measurements near saturation to increase accuracy of the estimation.

The RMSE of the TF models matched the error threshold of the TDR probes (~0.05) and fit substantially better than the SSL models. Inverse simulation of field lysimeter experiments conducted by Schwärzel et al (2006a) also estimated parameters that better fit field observations of soil moisture than parameters from laboratory derived retention curves. Their parameters from inverse simulation of laboratory evaporation experiments (transient laboratory, TL) also performed substantially better

than steady state experiments (TF > TL >> SSL) (Schwärzel et al 2006a). The TF used here model did not perform well during rain events (e.g., hours 1400 to 1600) and under-predicted soil moisture; although Schwärzel et al (2006b) had the opposite problem, soil moisture was over-estimated. It was possible that this could be due to the difference in the α value which reflects an air-entry pressure that is not representative of wetting and drying processes. Parameters from inverse simulation were also unable to describe soil moisture beyond the calibration range; Schwärzel et al (2006a) reported similar difficulties predicting beyond the calibration.

The observed shortfalls may be a result of missing processes, as is suggested by the slope of the observed vs. simulated regression being significantly different from 1 (Table 2-4). The residuals of the regression were not normally distributed, distinct patterns were observed. The TF simulation over-estimate moisture in the dry range and under estimated moisture near saturation. Additionally, over-estimation in a looped pattern was observed. Additional process, such as hysteresis and dual porosity, may need to be accounted for. Hayward and Clymo (1982) have remarked on the dramatic effect that hysteresis can have on water content; since then several authors have observed it when building retention curves (da Silva et al 1993; Naasz et al 2005; Londra 2010; Price and Whittington 2010; McCarter and Price 2014). Furthermore, (Taylor and Price 2015) observed hysteresis with the dataset used for this study when plotting soil moisture in the top 5 cm against water table depth. If hysteresis is a process that is not accounted for within the calibration period, then α would represent an aggregate of the wetting and drying processes rather than the actual process.

Hayward and Clymo (1982) highlight two major pore systems: the interfoliar space created by overlapping branches, and the intracellular spaces associated with hyaline cells. As such, the assumption of unimodality of the pore-size distribution in the VGM would be violated, as suggested by Price et al (2008). Dettman et al. (2014) found a second pore domain at ~-400 cm of pressure, which coincides with the range of pressures at which hyaline cells drain (Lewis 1988). Pressures observed in this study are insufficient to drain hyaline cells; which would suggest a single porosity model should suffice. Alternatively, Weber et al. (2017b) found evidence of a triple porosity model where the first mode encompasses the inter-plant space (ψ > -10 cm); the second being the intra-plant space (-10 to -100 cm); and the third being the intact and skeletal hyaline cells (-100 to -300 cm).

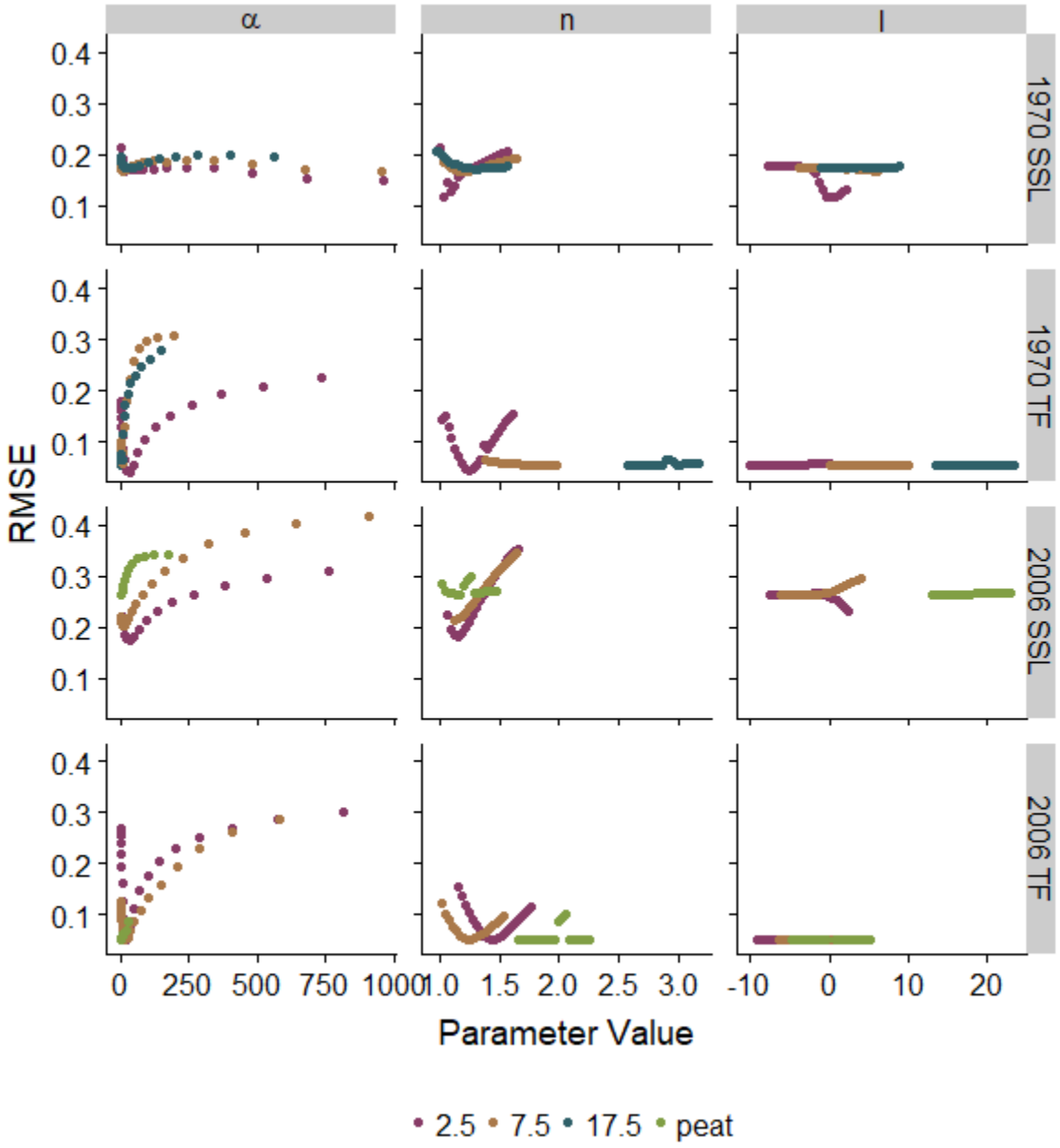

Figure 2-7: Sensitivity Analysis

Sensitivity analysis of all profiles and methods for all fit parameters. Trends in α were stable as such it was limited to values below 1000 for clarity.

Table 2-4: Regression coefficients and p-values of observed and simulated soil moisture

The p-value indicates whether the slope or intercept is statistically different from 1 or 0, respectively.

Method	Plot	Slope		Intercept		R^2
		coefficient	p-value	coefficient	p-value	
SSL	1970	0.81	>0.001	0.25	>0.001	0.84
SSL	2006	0.76	>0.001	0.36	>0.001	0.7
TF	1970	1.14	>0.001	-0.11	>0.001	0.94
TF	2006	1.05	>0.001	-0.03	>0.001	0.91

2.4.3 Limitations and error

Parameterization from SSL and TF modeling experiments can be restricted by a limited observation range to which they were fit, compromising realism and accuracy (van Genuchten et al 1991; Šimůnek et al 2009). The narrow range of θ-ψ observation was a major limitation to confidently estimating parameters in this study. Aside from potential methodological errors in steady state laboratory experiments, the pressure range is limited to a range where moss is not stressed (Hayward and Clymo 1982). A restricted pressure range is not an issue for managed systems (*Sphagnum* fibre farming), however, it would be important for predictions where the pressure range is unknown (drought). Similarly, parameter estimation in the lower layers of the TF models suffered from being fit to a small range of observations and was reflected in the increasing magnitude of the confidence intervals with depth. Laboratory evaporation experiments (Schelle et al 2013; Dettmann et al 2014; Weber et al 2017b) may be best suited to build retention curves because the entire moisture range can be captured.

The consequence of parameters being highly correlated creates an increase in uncertainty and non-uniqueness because changes in one correlated parameter result are compensated by a change in the correlated parameter (van Genuchten et al 1991; Šimůnek and Hopmans 2002). The correlation of α and n in the moss (<-0.9) and peat (>0.9) from inverse simulation provide further evidence that the model is ill-posed, and may result in error when predicting soil moisture near or beyond the soil moisture range of the calibration period (Kool et al 1987). Schwärzel et al (2006a) overcame similar

limitations by specifying that correlated parameters were strictly fitting parameters with no physical basis and by limiting their application to the range of observations to which they were fit. By extension, the TF parameters from this study can be used for prediction where the moisture range is not expected to go beyond calibration. To better define correlated parameters one of them could be fixed, which can be done by obtaining a physical measurement or through stepwise parameter estimation (van Genuchten et al 1991; Šimůnek and Hopmans 2002; Schwärzel et al 2006a; Šimůnek et al 2012). High correlation was also observed in RETC curve fitting, as such similar strategies can be applied.

As previously discussed, parameter estimation using RETC and Hydrus is limited by the estimation algorithm, it is recommended that several initial conditions are used to properly estimate parameters (van Genuchten et al 1991; Šimůnek et al 2009). A thorough exploration of the impact of initial conditions was not done due to the complexity associated with estimating parameters for a multi-layered system. Daniel and Woods (1980) recommend that the initial parameter estimates of a local solver should approximate the real value, as such different initial conditions based on newly and previously estimated parameters were compared. Two sets of initial estimates were assessed, the first were the parameter estimates from RETC, the second were from inverse simulation of evaporation experiments (ALT) by Weber et al (2017b). α values remained similar between the ALT and TF; however, ALT values had more uncertainty (Table 2-2). Additionally, the estimates of n from the ALT model were more realistic and decreased with depth, as is expected with an increase in bulk density (Sherwood et al 2013; Moore et al 2015). The largest difference was in the pore connectivity parameter l. ALT parameters were all positive and had a much smaller range, notably the 1970 profile. Despite the ALT parameters being more reasonable than those of TF, the confidence intervals were equally large. The MAE, ME, RMSE, NSE, and KGE' of the 2006 ALT profile were virtually identical to the 2006 TF profile. Alternatively, the error metrics of the 1970 ALT profile showed that it performed worse than 1970 TF profile (Table 2-3). Multiple sets of valid initial conditions support the idea that the model is ill-posed; however, that does not discount its usefulness within the calibrated range. Using global search methods would better be able to explore the parameter space (*e.g.* Weber et al 2017b; Weber et al 2017a).

Some authors have discretized the profile in 5 cm increments to the dimensions of soil cores (Price and Whittington 2010; McCarter and Price 2014; Gauthier et al 2018). Conversely, other authors have estimated or aggregated parameters across layers within a profile (Moore and Waddington 2015; Golubev and Whittington 2018). Where detailed soil moisture isn't a concern

there is no issue; however, where accurate moisture is critical it may become problematic. In this study it was assumed that VGM parameters would change with depth due to changes in bulk density and decomposition. The profiles were discretized to match instrumentation or sampling methods that aim to capture vertical heterogeneity. Further work assessing the discretization of soil properties within models is needed.

2.5 Conclusion

The objective of this study was to determine which parameters best described soil moisture dynamics at the field scale, when determined by curve fitting to SSL experiments or inverse simulation to TF observations. SSL parameters consistently underestimated soil moisture in the field, despite being in agreement with literature values. Parameters estimated by inverse simulation were adequately able to described field scale soil moisture; however, the fit was generally poor when simulated soil moisture exceeded the observed range used for calibration. As such the use of parameters determined with TF simulations would be more useful for predicting soil moisture in managed peatlands where extreme conditions are not allowed to go beyond the calibration. In order to predict soil moisture in a more robust manner a different model that accounts for other processes may be required. We have identified several reasons why the VGM may be inadequate to represent field soil moisture

1. The slope and intercept for the regression of the observed and simulated soil moisture is significantly different from one and zero, suggesting that the model does not account for all pertinent processes.
2. The non-random distribution of the residuals alludes to other processes that should be considered, such as hysteresis and multiple porosities.

Parameterization of peatland retention with the goal of predicting soil moisture under a large variety of condition should be done with deliberate laboratory or field evaporation experiments where a large range of soil moisture can be observed. However, if the intended use of the model is for managing *Sphagnum* fibre farming operations or other scenarios where the water table is maintained near the surface, a limited calibration, like the one used in this study, is acceptable.

Chapter 3
Assessment of different approaches to representing the soil water retention curve in regenerated *Sphagnum* moss

3.1 Introduction

The management of restored and industrial peatlands could benefit from accurately predicting water exchanges to meet biomass production and carbon sequestration goals (Schwärzel et al 2006a; McCarter and Price 2015; Brown et al 2017). Modeling, hence predicting hydrological response of mosses, has not been done effectively at the field scale because of the difficulty of acquiring an adequate dataset for parameterization (Schwärzel et al 2006a; Chapter 2). Inverse simulation of parameters to data from transient field experiments have been able to define models that can adequately simulate the middle range of soil moisture, however model accuracy is limited at the extremes (Schwärzel et al 2006a; Schwärzel et al 2006b; Chapter 2). In Chapter 2 it was hypothesized that including additional processes, such as hysteresis or dual porosity, in the model could better simulate soil moisture at the edges of the calibration range.

Unsaturated hydraulic models require the relationships between soil water pressure (ψ), soil moisture (θ), and conductivity (K) to be defined. There are several parametric models (approaches) that can be used to define the soil water retention ($\theta(\psi)$) and hydraulic conductivity ($K(\psi)$) curves. The most common approach that is used in peatlands is the van Genuchten – Mualem (VGM) equation; it has been successful at characterizing laboratory retention and hydraulic conductivity curves (Schwärzel, Šimůnek, Stoffregen, et al., 2006; Schwärzel, Šimůnek, Van Genuchten, et al., 2006; Chapter 2). Recently, evidence has been presented that more complex retention curve approaches that including additional processes, such as a multi-modal pore domain, can improve model fit (Weber et al 2017a).

Soil moisture hysteresis is the process in which soil moisture will differ at the same pressure depending on the previous moisture content and whether it is drying or wetting. In *Sphagnum* moss and peat soil, hysteresis has been observed in laboratory (Hayward and Clymo 1982; da Silva et al 1993; Naasz et al 2005; Londra 2010; Price and Whittington 2010; McCarter and Price 2014; Gharedaghloo and Price 2018) and field studies (Taylor and Price 2015). Hysteresis has been shown to be an important process to include when modeling the vadose zone of mineral soils (Bashir et al 2016), however it has yet to be included in models of organic soils. Hysteresis is generally attributed

to non-uniformity in the size of pores ("ink bottle effect"), difference in contact angle, depending on the advance or retreat of water (raindrop effect), and entrapped air (Tuller and Or 2004). In addition to the aforementioned processes, organic matter within soil has also been shown to have a dramatic impact on the contact angle by altering the hydrophobicity during drying and wetting (Michel et al 2001; Naasz et al 2008; Diamantopoulos et al 2013). In many cases *Sphagnum* and peat (up to 100% organic) can switch from hydrophilic to hydrophobic, increasing the magnitude of hysteresis (Michel et al 2001; Schwärzel et al 2006b). Naasz et al. (2008) observed a difference in contact angle of up to 20% between horticultural peat drying and wetting between -30 and -3222 cm of water pressure. Additionally, Gharedaghloo and Price (2018) observed a difference in contact angle of 89° between water-wet and air-wet peat. It is likely that excluding hysteresis in peatland unsaturated flow models could lead to poor estimations of soil moisture under wetting and drying conditions. Kool et al. (1987) have mathematically represented hysteresis in the soil water retention curve by defining the main drying and wetting branches with the VGM. Scanning curves are all possible wetting and drying paths between the main drying and wetting branches (Scott et al 1983). A scaling equation is used to scale the main drying or wetting curve to represent the scanning curves, which is dependent on drainage or imbibition. The original implementation of hysteresis has been known to occasionally exhibit a pumping effect, where the scaling equation assigns the scanning curve to an unrealistic portion of the retention curve resulting in an over or under estimation of soil moisture (Kool and Parker 1987). The pumping effect is an error which occurs at reversal points, when drying switches to wetting or vice versa, and the scanning curve has not ended on one of the main branches (Zhang et al 2014). Parker and Lenhard (1987) have composed an alternative scaling equation; which uses historical reversal points within the calculation to prevent the pumping effect.

The VGM assumes that the soil matrix has a single pore domain, however *Sphagnum*-based organic soils can have several domains either within the plant or between plants (Hayward and Clymo 1982; Weber et al 2017a). Pore domains closest to saturation represents the network in which water moves and drains easily; this is the active porosity (Rezanezhad et al 2012; Weber et al 2017a). The second pore domain accounts for the inactive porosity (Rezanezhad et al 2012). *Sphagnum* mosses have intact or partially decomposed hyaline cells that play a role in water storage (Hayward and Clymo 1982). These pores represent part of the second domain, which also includes other partially closed or dead-end pores, that do not contribute to flow, but can drain or refill (Rezanezhad et al 2012). In *Sphagnum* mosses, drainage of the second domain is associated with the diameter of the pores, such as the opening in the hyaline cells, and drainage has been found to occur between -100 to

-600 cm of pressure (Hayward and Clymo 1982; Lewis 1988; Dettmann et al 2014; Weber et al 2017a). Some pore-water within the second domain is considered immobile (Rezanezhad et al 2012) and may only be accessible through diffusion and vapour flow (Weber et al 2017a). Weber et al. (2017a) has suggested that an additional domain can exist near saturation to account for macropores in *Sphagnum* mosses, however previous work suggests that it's inclusion is not always necessary (Dettmann et al 2014). Conversely, representing macropores with dual porosity in drained peat soils has produced better results than unimodal approach (Dettmann et al 2014; Wallor et al 2018). The implementation of multiple porosities in organic soils has typically been represented by defining a mobile and immobile region (Rezanezhad et al 2012; Rezanezhad et al 2016; Gharedaghloo and Price 2018). However, it can also be achieved by having a weighted VGM equation for each domain, where each domain is a separate mode within the pore size distribution (Durner 1994). The Durner (1994) representation of dual porosity can also be labeled as bimodal in reference to a pore-size distribution with two peaks; the mobile and immobile regions are not specified. Additionally, multi-modal porosity approach can be used to add flexibility to VGM to describe non-uniform single porosity domains (Durner 1994). The implementation of a model that includes either macropores or a representation of a non-uniform pore distribution near saturation may be able to overcome limitations found in Chapter 2.

Model simplicity is valued because it decreases the uncertainty within the parameters and makes achieving a unique solution that represents the dominant processes of a system easier (Carrera and Neuman 1986; Snowling and Kramer 2001). As such, a simple model is less at risk of being ill-posed (Hopmans et al 2002). An ill-posed model is problematic because inverse simulation can generate multiple parameter sets (non-unique), multiple parameter sets can be used to solve a forward simulation (non-identifiable), and small variations in input have a large effect on the output (stability) (Carrera and Neuman 1986). Complex models are attractive because additional parameters increased model flexibility, which can results in less error (Snowling and Kramer 2001; Hopmans et al 2002; Peters et al 2011). However, this will result in a more complex parameters space that can have more local minima, thus increasing the likelihood of a non-unique solution. This can be mitigated by using prior information to limit the parameter space or fix parameters (Šimůnek and Hopmans 2002). The appropriate approach will be complex enough to represent all of the pertinent processes (Kool et al 1987), yet simple enough to have unique parameters and be applicable beyond the calibration (Snowling and Kramer 2001). As such, a simpler model may be more appealing even though it has more error (Russo 1988). Model error can be more pronounced at the wet and dry ends of the curve if

the wrong approach was selected (Kosugi et al 2002); in Chapter 2 error was greatest in these regions. The goal of using more complex approaches, which include for hysteresis and dual porosity, is to reduce error in the wet and dry range.

Chapter 2 showed that inverse simulation, with transient field data, generated a better VGM parameter set than steady state laboratory curve fitting. However its ability to predict soil moisture extremes during wetting and drying events at the field scale using a relatively simple approach is limited (Schwärzel et al 2006a; Schwärzel et al 2006b; Chapter 2); more complex approaches may be able to better represent field soil moisture dynamics. The goal is to simulate soil moisture dynamics in the moss layers using inverse simulation with additional parameters that account for hysteresis in the water retention curve and the dual porosity character of peat. Parameters for each approach will be estimated through inverse simulation. Model performance will be assessed using field-scale soil moisture regimes of regenerated *Sphagnum* moss using standard error metrics.

3.2 Methods

3.2.1 Study site and sample preparation

Field and laboratory observations were collected and published by Taylor and Price (2015); a complete description of the site and methods is available in the original publication. Briefly, the study site is a cut-over peatland characterized by alternating raised baulks and lowered trenches. Spontaneous recolonization of *Sphagnum* mosses occurred in the trenches after abandonment in 1970. Beginning in 2004 *Sphagnum* fibre farming plots were established by removing all of the vegetation and spreading *Sphagnum* diaspores every two years until 2010 (Landry and Rochefort 2009). Plots are identified by the year in which colonization or planting occurred. Each plot was underlain by old cut-over peat, where the moss was of variable thicknesses and reflected the time since re-establishment (Taylor and Price 2015). The original study had three 1970 plots, however only one was instrumented, where in this study 1970 will represent the 1970-C plot in the original. Water table, meteorological conditions, and soil moisture were recorded every hour. Soil moisture was measured using triplicate CS605 TDR probes installed at depths of 2.5, 7.5, 12.5, and 17.5 cm; and 2.5, 7.5, and 12.5 cm for the 2006 and 1970 plots, respectively. Saturated hydraulic conductivity and porosity were determined in the laboratory using cores 10 cm in diameter and 5 cm in height (Taylor and Price 2015).

3.2.2 Determination of soil hydraulic parameters and model setup

Five approaches were used to simulated soil moisture dynamics in the 1970 and 2006 moss profiles; three of which were calibrated during the wet and dry period and two only during the dry period, for a total of eight parameter sets (Table 3-1; Appendix C). Briefly, these included the VGM (Chapter 2), two implementations of the VGM with hysteresis (Kool and Parker 1987; Parker and Lenhard 1987), and two parameterizations of the of bimodal dual porosity approach (Durner 1994). Parameterization of each approach was done using inverse simulation in Hydrus-1D v.4.16 (Table 3-1). Calibration was done for 20 days of the 82-day observation period; two periods were examined to assess the impact on parameter estimation (Table 3-2). The first calibration period was selected to capture the largest variation in soil moisture across all layers (hour 800 to 1280); approaches calibrated in this period will be marked with the subscript 'dry'. An alternate calibration period captured the wet period with large fluctuations in soil moisture (hour 0 to 480); approaches calibrated in this period will be marked with the subscript 'wet'. The model domain for the 1970 and 2006 profiles were 47 and 58 cm in height, respectively (Figure 3-1) and node spacing was 0.5 cm. In the 1970 profile, layers 1, 2 and 3 represent *Sphagnum* moss 5, 5 and 10 cm thick, respectively, and underlain by cutover peat (layer 4). The 2006 profile had *Sphagnum* moss in layers 1 and 2 (each 5 cm thick), and layer 3 was cutover peat. Water table observations were used to define a variable pressure head for the bottom boundary condition. The upper boundary condition was characterized as atmospheric and was defined with observations of precipitation and estimates of potential evapotranspiration (Taylor and Price 2015). Potential evapotranspiration was estimated using the Priestly-Taylor method (Priestley and Taylor 1972); the evaporability parameter (*alpha*) was set to 1.26 (Price 1992; Petrone et al 2008). In Hydrus, the soil water atmospheric vapour equilibrium (*hCrita*) defines the pressure at which evaporation capacity is exceeded (Šimůnek et al 2009). An *hCritA* of -10 000 cm was used because it is the pressure at which Thompson and Waddington (2008) and Goetz and Price (2015) suggest soil vapour equilibrium occurs. Initial soil moisture conditions were determined by TDR observations and water table depth at the first modelled timestep.

The first approach tested used the VGM equation and is defined as:

$$S_e = \frac{1}{(1 + |\alpha\psi|^n)^m} \quad (1)$$

$$S_e = \frac{\theta - \theta_r}{\theta_s - \theta_r} \quad (2)$$

$$K(S_e) = K_s S_e^l \left(1 - \left(1 - S_e^{1/m}\right)^m\right)^2 \quad (3)$$

where S_e is the effective water content, ψ is the pressure head [L], K_s is the saturated hydraulic conductivity [L T^{-1}], and θ, θ_r, and θ_s are the water content, residual water content, and saturated water content, respectively. The parameters α [L^{-1}], n and l are fitting parameters that represent the inverse of the approximate air-entry pressure, width of the pore size distribution, and the pore-connectivity, respectively. The parameter m is calculated as 1-1/n.

The second and third approaches implement van Genuchten - Mualem with hysteresis and are defined identically to the VGM with the exception that α in Equation 1 is defined for the drying and wetting branches as α and α_W, respectively. If α approximates the pressure at which the largest pores start to drain, α_W approximates the pressure at which those same pores start to fill. For the wetting branch, α_W is restricted to being equal or greater than α of the drying branch (Šimůnek et al 2009). To represent hysteresis, scanning curves and reversal points are determined by using scaling equations. The original formulation of the hysteresis scaling equations by Kool and Parker (1987) is susceptible to pumping error (HYST pump), however, Parker and Lenhard (1987) formulated an alternate that avoids pumping (HYST no pump). The wetting branch of the hysteresis curve has a separate saturated water content ($\theta_s W$) and hydraulic conductivity ($K_s W$), and an air-entry value (θm) (Šimůnek et al 2009). Assuming that saturated water content is equal between the main wetting and drying curves, they all become fixed: $\theta m = \theta_s W = \theta_s$ and $K_s W = K_s$ (Šimůnek et al 2009). The Fourth and fifth approaches (Durner 1994) are represented by:

$$S_e = \sum_{i=1}^{k} w_i \left(\frac{1}{(1 + |\alpha_i h|^{n_i})^{m_i}}\right) \quad (4)$$

where i denotes the pore system and w the weight of each mode, where the sum of w_i is 1. k is equal to 2 to limit the number of modes to two. The hydraulic conductivity model by Mualem (1976) is reformulated (Priesack and Durner 2006) as:

$$K(S_e) = K_s \left(\sum_{i=1}^{k} w_i S_{e\,i}\right)^l \left(\frac{\sum_{i=1}^{k} w_i \alpha_i \left(1 - \left(1 - S_{e_i}^{1/m_i}\right)^{m_i}\right)}{\sum_{i=1}^{k} w_i \alpha_i}\right)^2 \quad (5)$$

Due to the limitation of the number of parameters that can be fit in Hydrus, the parameter l was fixed in all dual porosity approaches. The parameter l was set based on the estimate from the respective unimodal VGM approach, layer, and profile. The data being fit represent the wet end of the curve; as such, fixing l should not greatly impact the estimation of other parameters (Dettmann et al 2014). One dual porosity approach allowed α_1, α_2, n_1 and n_2 to vary freely (DUAL free); whereas the other only allowed α_2 and n_2 to vary, to explicitly simulate macropores (DUAL fixed). The α_1 and n_1 values for DUAL fixed corresponded to those estimated by Weber et al (2017a) in layers of equivalent depth of the VGM3 approach, from the original publication. The parameters α_1 and n_1 from the DUAL approaches are synonymous with α and n from the VGM and HYST approaches.

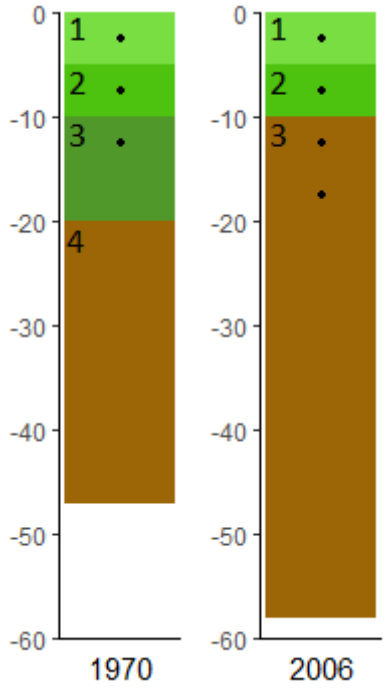

Figure 3-1: Model domain and TDR location

Model domain for the 1970 and 2006 proles; the green area is regenerated moss and the brown cut-over peat. Layer numbers are in the upper left corner and the black dots are the nodes used to compare to the field observations of soil moisture.

3.2.3 Model Validation and Performance

Model validation was done by simulating each approach for the entire 82-day period, with parameters from their respective calibration period. The respective calibration period for the wet and dry

simulations was excluded from statistical analysis. Model validation performance was assessed using mean average error (MAE), root mean square error (RMSE), mean bias error (ME), Nash-Sutcliffe efficiency (NSE), and modified Kling-Gupta efficiency (KGE'); a more complete description of their formulation and purpose can be found in Chapter 2. The best model was determined by using the Bayesian information criterion (BIC), which penalizes models for the number of parameters, where lower numbers are associated with a better fit and fewer parameters. Taylor diagrams were used to graphically represent the standard deviation and correlation to facilitate a visual comparison of the different models (Taylor, 2001). As in Chapter 2, regression of the observed and simulated soil moisture was performed and a t-test was conducted on the slope and intercept to evaluate model consistency and bias, respectively.

Table 3-1: Fitting parameters and parameter space for each approach

Overview of parameters used for each parameter where 'x' represents a fitted parameter and '-' represents fixed parameters. Blank spaces signify that the parameter was not used in that model. The upper and lower bounds delineate the limits of the parameter space. The equations that define the model are denoted in the equations column; the scaling equation for hysteresis is noted. The calibration column specifies the time range in hours of the observations that were used for calibration.

Approach	α (cm^{-1})	n	l	w_2	α_2 (cm^{-1})	n_2	α_W (cm^{-1})	Equations	Calibr
VGM $_{dry}$	x	x	x					1-3	800-
VGM $_{wet}$	x	x	x					1-3	0-4
HYST no pump $_{dry}$	x	x	x				x	1-3[1]	800-
HYST pump $_{dry}$	x	x	x				x	1-3[2]	800-
HYST no pump $_{wet}$	x	x	x				x	1-3[1]	0-4
DUAL free $_{dry}$	x	x	-	x	x	x		4-5	800-
DUAL fixed $_{dry}$	-	-	-	x	x	x		4-5	800-
DUAL free $_{wet}$	x	x	-	x	x	x		4-5	0-4
Upper bound	100	10	20	1	50	10	0		
Lower bound	0	1.001	-5	0	0	1.001	1000		

[1] Modified hysteresis scaling equation to prevent pumping effect (Parker and Lenhard, 1987)

[2] Original hysteresis scaling equation (Kool and Parker, 1987)

Table 3-2: Soil moisture observation frequency during the wet and dry calibration periods

Profile	Layer	# of Observations	
		Wet	Dry
1970	1	480	480
1970	2	395	480
1970	3	30	480
2006	1	480	480
2006	2	405	446
2006	3	20	30

3.3 Results

Most estimates of α decreased with depth; estimates of n for the 2006 profile also decreased with depth in moss layers (1 and 2 as identified in Figure 3-1). However, the 1970 profile had the opposite trend (Table 3-3). In the top layer (1), parameter estimates between the 1970 and 2006 profiles were generally similar when they were fit with the same approach. This trend did not occur in other layers. On average estimates of α_w were 4.7 and 3.3 times larger than α for the 1970 and 2006 profiles, respectively in the HYST no pump $_{dry}$ but was not the case for HYST pump $_{dry}$ and HYST no pump $_{wet}$. Additionally, estimates of α for HYST no pump $_{dry}$ were lower than those of VGM $_{dry}$, DUAL free $_{dry}$, and DUAL fixed $_{dry}$. Interestingly, α in layer 1 of the 2006 profile in the DUAL free $_{dry}$ approach was smaller than that of the 1970 profile. Both DUAL free $_{dry}$ and DUAL fixed $_{dry}$ had similar estimates for α_2 and n_2 for the 2006 profile. Generally, estimates of w_2 were above 0.5; thus, weighting the second porosity higher. There were no trends for parameter estimates with depth between the 1970 and 2006 profiles from the majority of parameters from the wet calibration period (not shown).

Parameter correlation of unimodal approaches, from inverse simulation, was minimal and only α and n within each layer were highly correlated (~±0.95) for VGM $_{dry}$ and HYST no pump $_{dry}$ approaches (Appendix D). No parameters were highly correlated for the HYST pump $_{dry}$ approach, however many were moderately correlated (~±0.5). Numerous parameters within both dual porosity approaches were highly correlated within each layer.

Table 3-3 Estimated parameters

Estimated parameters from inverse modeling for all models calibrated with the original calibration period for each profile. Parameter estimates from the alternate calibration period were not included to increase readability.

Plot	Method	Layer	α (cm^{-1})	n	l	w_2	α_2 (cm^{-1})	n_2	α_W (cm^{-1})
1970	DUAL free $_{dry}$	1	0.47	1.93	-2.85	0.52	0.03	2	
1970	DUAL free $_{dry}$	2	0.1	2.26	1.1	0.57	0.01	1.51	
1970	DUAL free $_{dry}$	3	0.04	2.11	3.87	0.01	0.05	3.68	
1970	DUAL fixed $_{dry}$	1	0.55	2.36	-2.85	0.61	0.04	1.97	
1970	DUAL fixed $_{dry}$	2	0.33	2.04	1.1	0.98	0.06	1.79	
1970	DUAL fixed $_{dry}$	3	0.36	2.08	3.87	1	0.05	2.51	
1970	HYST no pump $_{dry}$	1	0.1	1.83	-2.85				0.6
1970	HYST no pump $_{dry}$	2	0.05	2.15	1.1				0.22
1970	HYST no pump $_{dry}$	3	0.05	2.87	3.87				0.2
1970	HYST pump $_{dry}$	1	0.52	1.28	-4.22				0.74
1970	HYST pump $_{dry}$	2	0.06	1.49	0.63				0.21
1970	HYST pump $_{dry}$	3	0.03	1.87	4.61				0.22
1970	VGM $_{dry}$	1	0.47	1.31	-5				
1970	VGM $_{dry}$	2	0.06	1.68	5				
1970	VGM $_{dry}$	3	0.05	2.87	18.38				
2006	DUAL free $_{dry}$	1	0.19	3.01	-4.11	0.49	0.03	1.72	
2006	DUAL free $_{dry}$	2	0.22	1.59	-1.46	0.57	0.02	1.27	
2006	DUAL free $_{dry}$	3	0.05	1.34	0.16	0.67	0	1	
2006	DUAL fixed $_{dry}$	1	0.55	2.36	-4.11	0.69	0.07	1.72	
2006	DUAL fixed $_{dry}$	2	0.33	2.04	-1.46	0.79	0.03	1.61	
2006	DUAL fixed $_{dry}$	3	0.05	1.87	0.16	0.79	0	1.03	
2006	HYST no pump $_{dry}$	1	0.1	1.87	-2.61				0.34
2006	HYST no pump $_{dry}$	2	0.13	1.29	-1.08				0.43
2006	HYST no pump $_{dry}$	3	0.01	2	17.92				9.48
2006	HYST pump $_{dry}$	1	0.24	1.25	-4.99				2.4
2006	HYST pump $_{dry}$	2	0.24	1.14	-1.2				1.53
2006	HYST pump $_{dry}$	3	0.02	1.12	19.05				0.08
2006	VGM $_{dry}$	1	0.26	1.46	-4.11				
2006	VGM $_{dry}$	2	0.18	1.23	-1.46				
2006	VGM $_{dry}$	3	0.01	1.96	0.16				

Between the profiles of each dry calibrated approach, the retention curves had a similar shape with the exception of DUAL free $_{dry}$ where the 2006 profile had higher water content between -15 to 0 cm of pressure (Figure 3-2). The retention curve for layer 2 of the 2006 profile drained quicker and more than the 1970 profile for all approaches.

HYST no pump $_{dry}$ was the best performing approach. During the first 750 hours, HYST no pump $_{dry}$ simulated θ higher than the observed values in layer 1, whereas all other models calibrated to the dry period underestimated soil moisture (Figure 3-2). Additionally, θ of HYST no pump $_{dry}$ was almost always within +/- 0.05 of the observed value in layer 1 during the first two wetting events. It adequately desaturated during the largest drying event (~ hour 1500) and subsequently rewets within +/- 0.05 in layer 1. The largest deviation of θ using HYST no pump $_{dry}$ occurred in layer 2 of the 2006 profile during the driest observed period (~ hour 1500).

HYST pump $_{dry}$, DUAL free $_{dry}$, DUAL fixed $_{dry}$, and VGM $_{dry}$ all perform similarly, too dry during wetting events and too wet during the driest period. The largest model residual was observed in layer 1 (Figure 3-2). Despite similar performance there were occasions where DUAL free $_{dry}$ and HYST pump $_{dry}$ performed differently. During the wet period (hours 0-480) DUAL free $_{dry}$ performed better. After the rain event following the driest period, HYST pump $_{dry}$ varied substantially more in layer 1 of the 2006 profile (~hour 1500).

Models with approaches calibrated in the wet period performed substantially worse than those calibrated in the dry period. In general, the moss layers of simulations calibrated to the wet period rapidly desaturated during drying events (Figure 3-2). VGM $_{wet}$ had the most error for all layers and profiles (Table 3-3). All models calibrated in the wet period have better initial wetting after the rain event around hour ~1600, however they do not have an acceptable match with the observed soil moisture during the subsequent wetting and drying events.

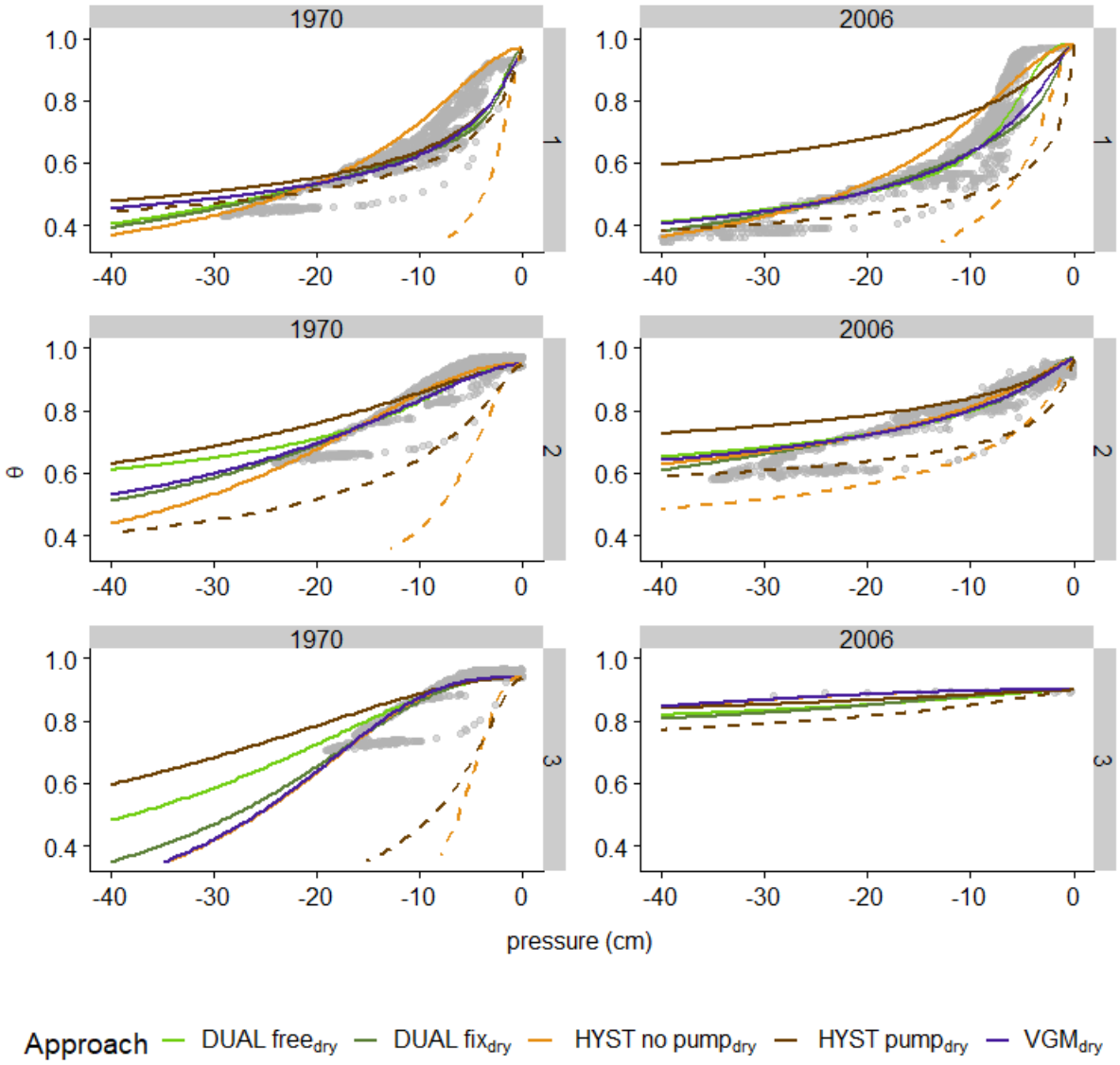

Figure 3-2: Soil water retention curves

Retention curves for all models calibrated in the original period overlain on the observed data. The dashed lines are the wetting curves for models with hysteresis. Pressure was assumed from a 1:1 relationship from the probe to the water table. Retention curves for the wet calibration period were not included for clarity.

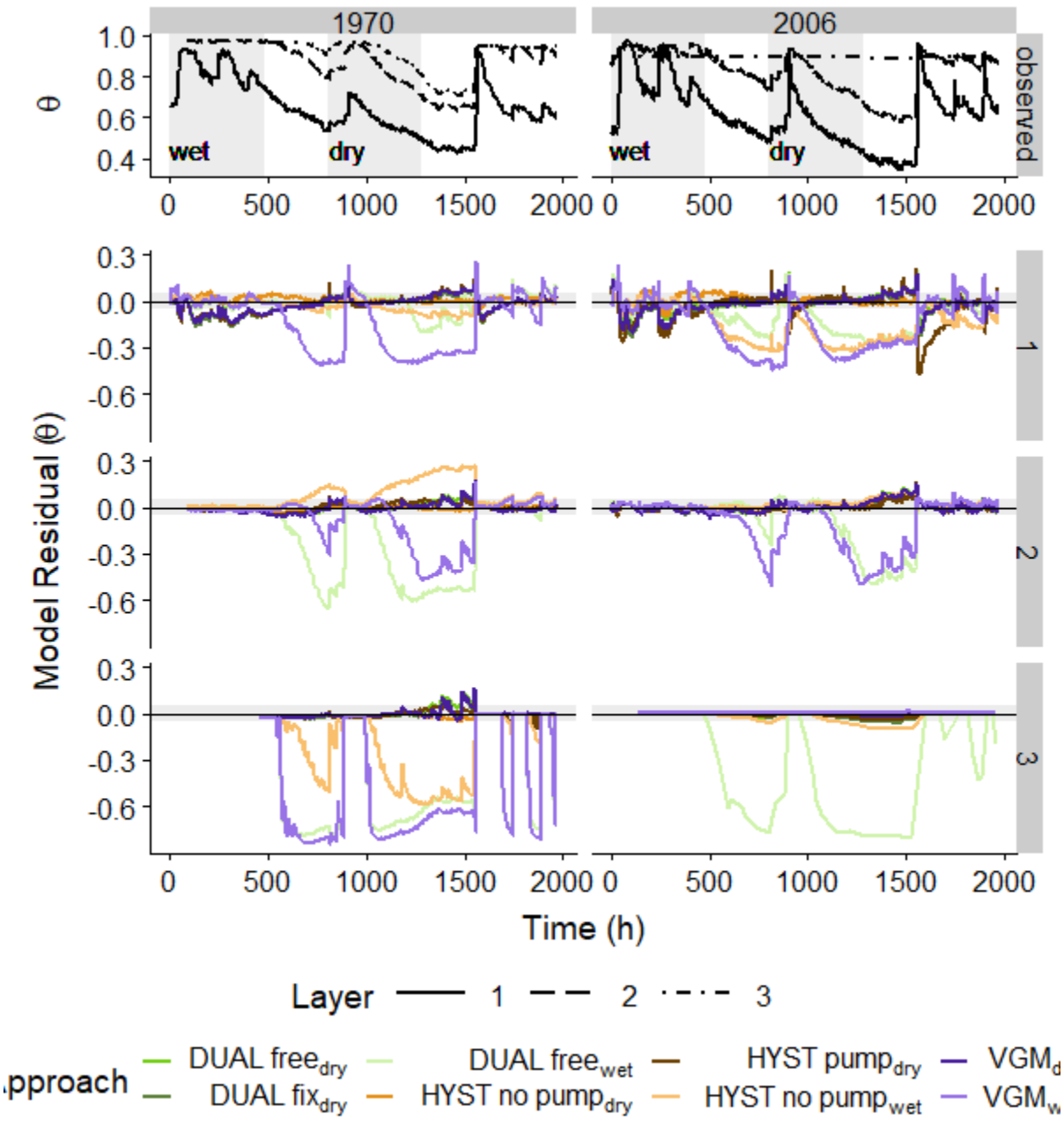

Figure 3-3: Observed soil moisture time series and simulated residual soil moisture

The top panel shows the observed soil moisture in the top three probes for each prole. The shaded grey areas on the observed data represent the two calibration periods. The bottom three panels show the residual of the modeled soil moisture for each layer of each prole, the shaded grey area represent ±0.05 around the observed soil moisture.

Table 3-4: Model error statistics

Plot	Approach	MAE	ME	RMSE	NSE	KGE'	R^2	BIC
1970	VGM $_{wet}$	0.28	-0.26	0.39	-4.81	-1.23	0.5	-8292
1970	VGM $_{dry}$	0.04	-0.02	0.05	0.91	0.93	0.96	-23769
1970	HYST no pump $_{wet}$	0.12	-0.06	0.2	-0.55	0.26	0.61	-14193
1970	HYST pump $_{dry}$	0.04	-0.02	0.05	0.91	0.92	0.96	-23909
1970	HYST no pump $_{dry}$	0.02	-0.01	0.02	0.98	0.97	0.99	-29901
1970	DUAL free $_{wet}$	0.26	-0.24	0.39	-4.59	-0.88	0.29	-8486
1970	DUAL fix $_{dry}$	0.04	-0.02	0.05	0.9	0.94	0.96	-23436
1970	DUAL free $_{dry}$	0.04	-0.01	0.05	0.90	0.94	0.92	-23440
2006	VGM $_{wet}$	0.18	-0.17	0.24	-1.09	-0.5	0.92	-8438
2006	VGM $_{dry}$	0.04	-0.01	0.06	0.89	0.89	0.95	-16533
2006	HYST no pump $_{wet}$	0.12	-0.09	0.16	0.06	0.04	0.95	-10801
2006	HYST pump $_{dry}$	0.05	-0.03	0.09	0.75	0.87	0.88	-14072
2006	HYST no pump $_{dry}$	0.03	0	0.04	0.93	0.94	0.97	-18009
2006	DUAL free $_{wet}$	0.13	-0.12	0.2	-0.45	0.08	0.87	-9512
2006	DUAL fix $_{dry}$	0.04	-0.02	0.06	0.88	0.91	0.94	-16142
2006	DUAL free $_{dry}$	0.04	-0.01	0.05	0.92	0.91	0.96	-17310

Overall the drying and wetting branches of the retention curves for HYST no pump $_{dry}$ encompassed virtually all of the observed soil moisture values (Figure 3-3). Notably, the drying branch of the HYST no pump $_{dry}$ curves in layer 1 captured all observations below 0 and -8 cm of pressure in the 1970 and 2006 profiles, respectively. The area between the drying and wetting branches of HYST pump $_{dry}$ were narrower than those of the HYST no pump $_{dry}$ and decreased more gradually (smaller *n* parameter) (Figure 3-3). As such, more of the observed points were not contained within the drying and wetting branches. In layer 1, VGM $_{dry}$, DUAL free $_{dry}$, and DUAL fixed $_{dry}$ curves were all very similar; with the exception of DUAL free $_{dry}$, which is wetter between -8 and 0 cm of pressure. Furthermore, VGM $_{dry}$, DUAL free $_{dry}$, DUAL fixed $_{dry}$, and drying branch of HYST no pump $_{dry}$ were also very similar with the exception of HYST no pump $_{dry}$ and DUAL free $_{dry}$

below -10 and -15 cm of pressure, respectively, in layer 2 of the 1970 profile. The divergence of DUAL free $_{dry}$ in 1970 layers 2 and 3 occurred where there was fewer field observation of soil moisture. All models, with the exception of HYST pump $_{dry}$, behaved in a similar manner when they were in the same range as the observed soil moisture values. The moisture range in the peat layer of the 2006 profile was inadequate to draw meaningful conclusions.

HYST no pump $_{dry}$ fit the best, having the highest correlation (0.99, 0.97), ME (0.005, 0.002), and lowest RMSE (0.02, 0.04) in the 1970 and 2006 profiles, respectively (Figure 3-4). Additionally, HYST no pump $_{dry}$ had the highest NSE and KGE', and lowest BIC within their respective profiles (Table 3-3). All models fit to the dry calibration were clustered together and had similar correlation (~0.96), ME (~-0.01), and RMSE (~0.05). Models within the cluster had similar NSE (~0.91, ~0.89), KGE' (~0.93, ~0.9), and BIC (~-23700, ~-16500) for the 1970 and 2006 profiles, respectively. Notably, DUAL free $_{dry}$ in the 2006 profile performed marginally better than the cluster (Figure 3-4). All models with approaches calibrated in the wet period had an ME less than -0.05 and an RMSE greater than 0.14. The NSE and KGE' of models calibrated in the wet period were less than 0.26; with the exception of 1970 DUAL fixed $_{wet}$, which had a KGE' of 0.6. The mass balance error for all simulations was less than 1%, with the exception of 1970 VGM $_{wet}$ (41%), 2006 HYST no pump $_{dry}$ (1.4%), and 2006 HYST pump $_{wet}$ (100%).

The residuals of the regression of the observed and simulated soil moisture were not normally distributed for all plots except 1970 HYST no pump $_{dry}$ (Figure 3-5). The 2006 profiles had residuals that suggested a bimodal distribution, with the exception of 2006 DUAL free $_{dry}$. All slopes and intercepts for the regression of the observed and simulated soil moisture of models calibrated in the dry period were within ± 0.07 and 0.08 of 1 and 0, respectively (Figure 3-6). However, they were all statistically different from the 1:1 line ($p << 0.05$), with the exception of the intercept for 1970 DUAL fixed $_{dry}$, and 2006 DUAL fixed $_{dry}$ (Table 3-4). The large sample size may be responsible for the small p-value (Sullivan and Feinn 2012). The slope and intercept of models calibrated in the wet period differed substantially different from those calibrated in the dry period (Appendix E). The distribution of the residuals of models from the dry calibration did not appear to be random (Figure 3-6). Common to all models calibrated in the dry period (excluding 1970 HYST no pump $_{dry}$) was an underestimation of soil moisture in the wet range in layer 1. In general, the deviation was more defined in the 2006 profile with the exception of DUAL free $_{dry}$, which had less deviation. Overestimation of soil moisture was observed in linear patterns and increased with increasing soil moisture in the 2.5 cm layer, with the exception of the HYST no pump $_{dry}$ profiles.

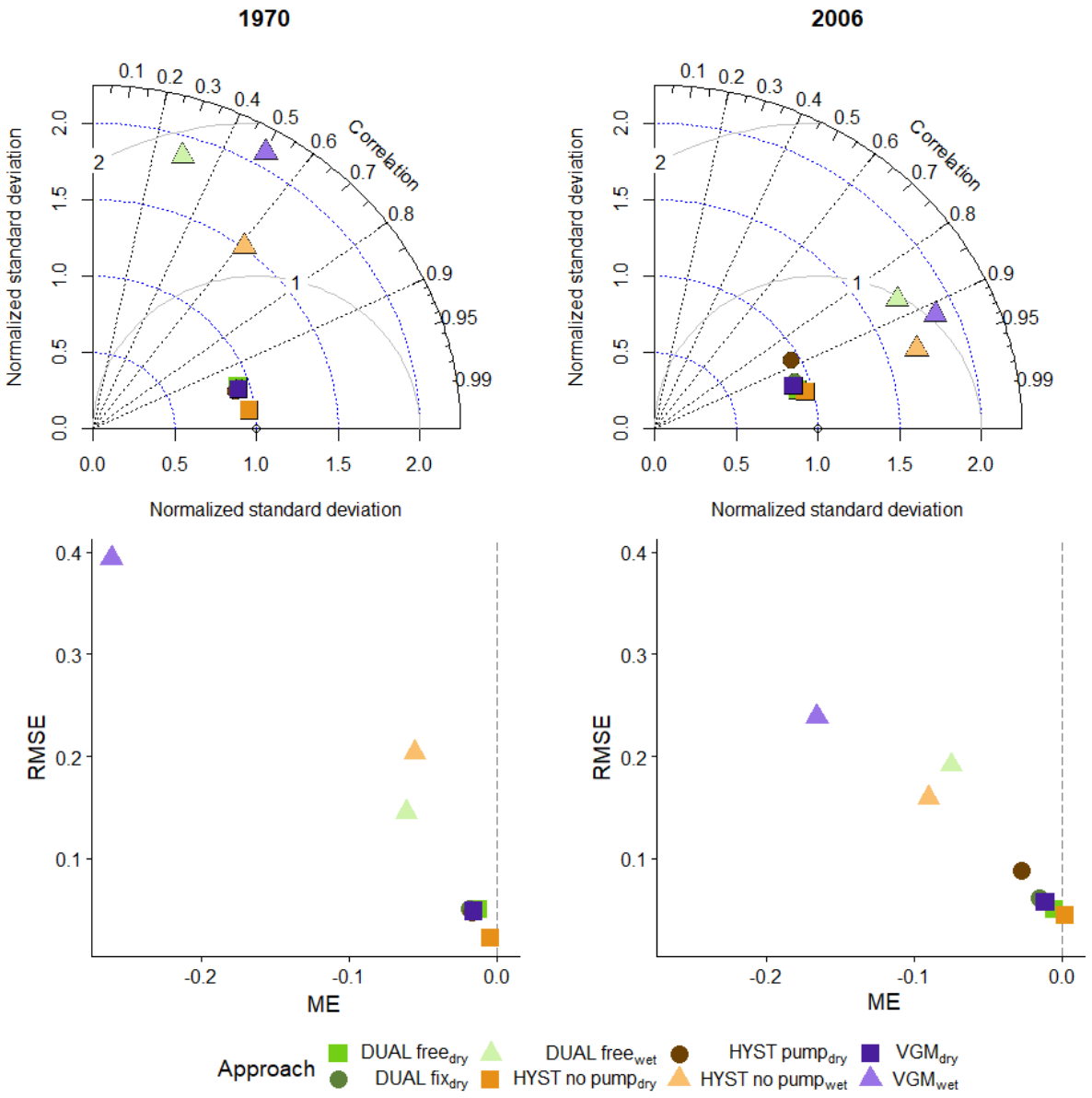

Figure 3-4: Taylor diagrams and model error

(top) Taylor diagrams for the performance of the combined calibration and validation period of all models. The arcs denote the normalized standard deviation, where a value of 1 is equal deviation of the model to the observations. The azimuth shows the degree of correlation between the observed and simulated soil moisture. (bottom) Visualization of error (RMSE) and bias (ME) for the validation period of all models.

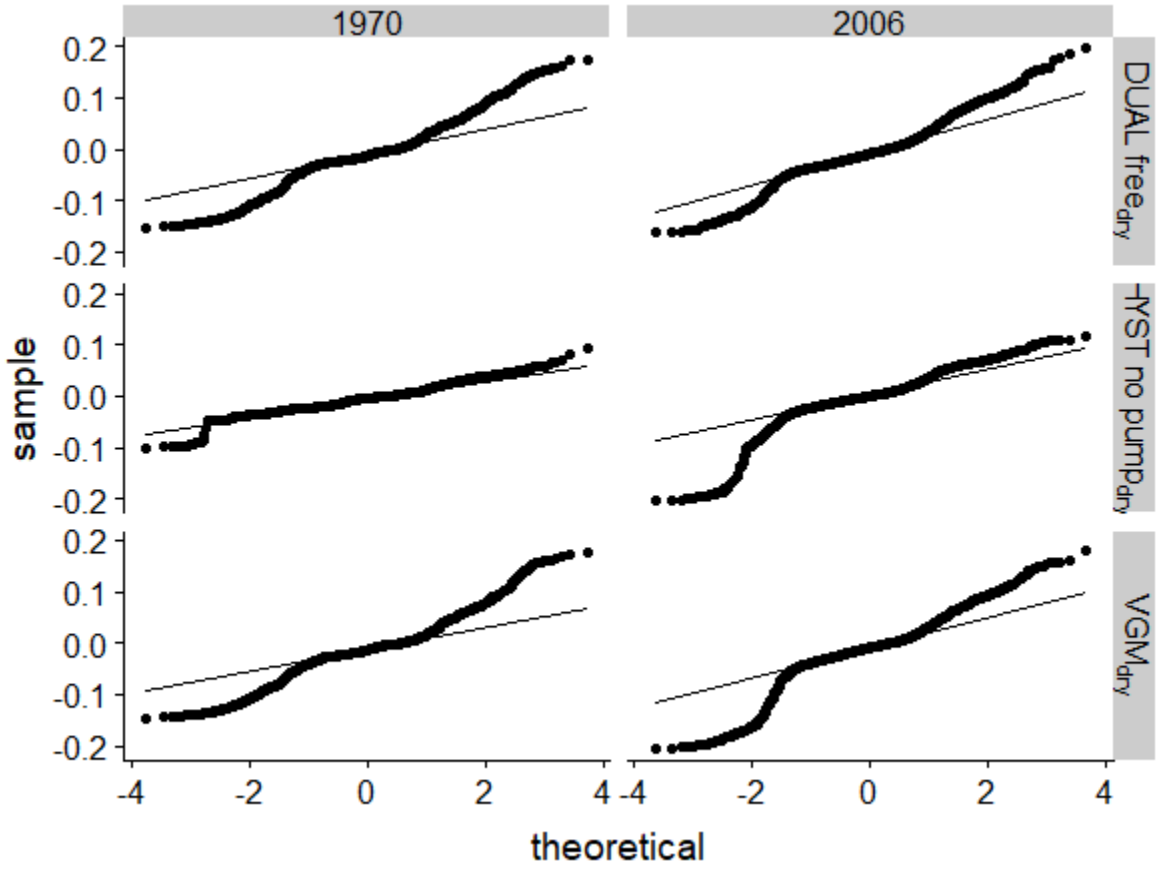

Figure 3-5: QQ plot of residuals from the regression of the simulated and observed soil moisture

DUAL $_{dry}$ and HYST pump $_{dry}$ were excluded because they behaved similarly to VGM dry. Models from the wet calibration period performed poorly and were omitted for brevity.

3.4 Discussion

3.4.1 Parameter Estimation

The soil moisture range to which models were calibrated to have a large impact on their ability to represent field soil moisture. Layers 2 and 3 in the wet calibration period, and layer 3 of the 2006 profile in the dry calibration period, were effectively always saturated during inverse simulation.

As such, the range of θ observed was inadequate to create retention curves that could represent drier periods (Figure 3-2). Although the VGM $_{dry}$, DUAL free $_{dry}$, and DUAL fixed $_{dry}$ models performed substantially better than those calibrated in the wet period, the predicted soil moisture was deviating from the observed during the driest period (Figure 3-2). Similarly, Schwärzel et al (2006a) reported that parameters from inverse simulation do not perform well in the dry range beyond the parameter calibration. It is suggested that the discrepancy could increase due to parameter non-uniqueness associated with a limited moisture range (Schwärzel et al 2006a). Conversely, HYST no pump $_{dry}$ performed very well during the driest period and may be able to adequately simulate soil moisture beyond the calibration range, however this should be validated.

Table 3-5: Regression coefficients and p-values of observed and simulated soil moisture

Plot	Method	Intercept		Slope		R^2
		coefficient	p-value	coefficient	p-value	
1970	DUAL free $_{dry}$	-0.01	>0.001	1.03	>0.001	0.91
1970	DUAL fix $_{dry}$	0	>0.001	1.02	>0.001	0.92
1970	HYST no pump $_{dry}$	-0.02	>0.001	1.03	>0.001	0.98
1970	HYST pump $_{dry}$	-0.03	>0.001	1.06	>0.001	0.93
1970	VGM $_{dry}$	-0.01	0.001	1.04	>0.001	0.92
1970	DUAL free $_{wet}$	0.69	>0.001	0.16	>0.001	0.09
1970	HYST no pump $_{wet}$	0.49	>0.001	0.41	>0.001	0.38
1970	VGM $_{wet}$	0.65	>0.001	0.24	>0.001	0.25
2006	DUAL free $_{dry}$	-0.03	>0.001	1.05	>0.001	0.92
2006	DUAL fix $_{dry}$	-0.01	0.113	1.03	>0.001	0.88
2006	HYST no pump $_{dry}$	-0.01	0.003	1.01	0.001	0.93
2006	HYST pump $_{dry}$	0.08	>0.001	0.93	>0.001	0.78
2006	VGM $_{dry}$	-0.03	>0.001	1.06	>0.001	0.9
2006	DUAL free $_{wet}$	0.39	>0.001	0.51	>0.001	0.75
2006	HYST no pump $_{wet}$	0.35	>0.001	0.56	>0.001	0.9
2006	VGM $_{wet}$	0.43	>0.001	0.49	>0.001	0.84

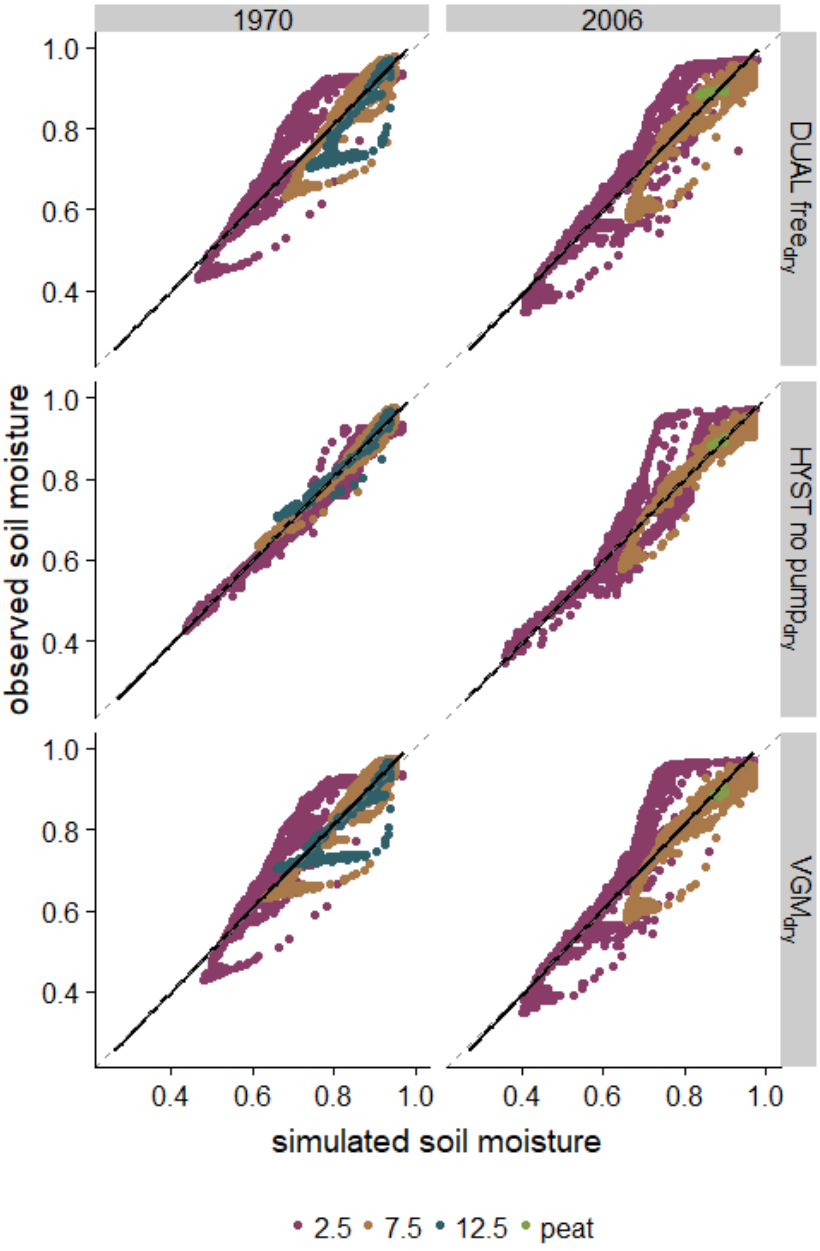

Figure 3-6: Regression of the simulated and observed soil moisture

Regression of the simulated and observed soil moisture. DUAL $_{dry}$ and HYST pump $_{dry}$ were excluded because they behaved similarly to VGM dry. Models from the wet calibration period performed poorly and were omitted for brevity.

Extrapolation beyond the observed values is further cautioned because values approaching θ_r were not observed (Figure 3-2). Proper estimation or definition of θ_r is important because it has been found to impact other parameters during the fitting process (Mualem 1976; Peters et al 2011; Moore et al 2015; Nijp et al 2017). Definitions of θ_r vary, however it is most consistently defined as the threshold beyond which water is considered immobile (Šimůnek et al 2009; Price and Whittington 2010; Rezanezhad et al 2012; Ghanbarian et al 2013; Weber et al 2017b). Inverse simulation in dry and wet conditions by Dettmann et al (2014) resulted in varying estimates of θ_r based on the minimum observed saturation. As such, sufficiently low pressure needs to be observed to estimate θ_r. In the absence of sufficiently low observed pressure, studies that have observed and fit θ_r provide a reference point for fixing the value (Moore et al 2015; Weber et al 2017b).

The drying curve of HYST no pump $_{dry}$ was able to more accurately represent air-entry pressure than other approaches (Figure 3-2). The scaling equations of the HYST no pump $_{dry}$ allow for the approach to represent the true main drying curve. In contrast all other approaches are an aggregate of wetting and drying processes. For mineral soils, Kool and Parker (1987) suggest that α_W can be estimated as double α if there are insufficient data. Within *Sphagnum* moss it was found that α_W could be between 3-5 times greater than α (Table 3-3). With more testing it may be possible to determine a ratio between α_W and α, for *Sphagnum* mosses. Discrepancies between the main wetting branch and the observed soil moisture in the 1970 profile suggest that the main wetting branch was not adequately captured. As such, the difference between α and α_W may decrease. It is likely that the moisture range experienced was not wide enough to parameterize a wetting branch that will accurately predict soil moisture lower than the observed values.

In general, the dual porosity approaches did not benefit model performance in any meaningful way, with the exception of layer 1 of the 2006 profile with the DUAL free $_{dry}$ approach (Figure 3-3). Although soil moisture was generally underestimated, the 2006 DUAL free $_{dry}$ retention curve follows the shape of the observation better than any other approach (Figure 3-3). The shape of the bimodal retention curves is similar to that of unimodal approaches, such as VGM $_{dry}$ and DUAL fix $_{dry}$ (Figure 3-3). If the curves are similar, α and n of the unimodal approach may be similar to α_1 and n_2 of the bimodal approach, this was not observed (Table 3-3). It is likely due to correlation of parameters during inverse simulation (Appendix D). Parameter correlation can result in a non-unique solution where several parameter sets can generate a similar retention curve, which is a risk of using more complex approaches (Šimůnek and Hopmans 2002). It is likely that there is increased error at

the edges of the calibration range when a model uses non-unique parameters because the middle of the range is where different parameter sets converge (Figure 3-3).

3.4.2 Model Performance

Based on the error metrics and the BIC, HYST no pump $_{dry}$ best simulated the observed soil moisture in both profiles (Table 3-3). Furthermore, the residuals of the regression of the observed and simulated soil moisture were normal or nearly normally distributed for the 1970 and 2006 HYST no pump $_{dry}$ approaches, respectively (Figure 3-5). The 1970 HYST no pump $_{dry}$ model had lower RMSE than the 2006, which is likely because of the superior characterization of the wet range in layer 1 (0 to -10 cm of pressure), thus it could better accommodate drainage and imbibition during and shortly after precipitation (Figure 3-2). A hysteresis retention curve represents all possible retention curves whereas other approaches represent an aggregate of wetting and drying processes. As such, the calibration of a hysteresis model should be more accurate than the VGM or a dual porosity calibration, where the situation may skew towards the wetting or drying curve with more observations.

Despite having slightly more error than DUAL free $_{dry}$ and DUAL fixed $_{dry}$ approaches, VGM $_{dry}$ was considered a better approach for the 1970 profile because it was simpler, thus scored a lower BIC (Table 3-3). The better performance of VGM $_{dry}$ over the models representing macropores (DUAL free $_{dry}$ and DUAL fix $_{dry}$) was also made by Dettmann et al (2014). The 2006 profile was better simulated with the DUAL free $_{dry}$ approach, and the distribution of the residuals no longer suggests a bimodal distribution (Figure 3-5). However, much of the wet range was still underestimated (Figure 3-3); it is possible that this was due to the curve being fit to an aggregate of the wetting and drying events. Had only the main drying curve been fit, it is likely that a second pore domain would have been more pronounced in 2006 DUAL free $_{dry}$, and revealed a separate domain for macroporosity, similar to Weber et al. (2017a).

The wet range was not well characterized by unimodal approaches in the 2006 profile because it is likely that there are macropores (Figure 3-3). The presence or absence in macropores in each profile is likely related to the different species composition. The 1970 profile is all *S. rubellum*, whereas the 2006 profile had a mix of *S. fuscum, S. rubellum,* and *S. magellanicum* (Taylor and Price 2015). Multi-modal approaches have been successfully fit to a mix of *S. rubellum* and *S. magellanicum* (Weber et al 2017a). Both *S. rubellum* and *S. fuscum* are small species that are densely clustered; as such the pore network contains a large proportion of small pores (Thompson and

Waddington 2008; McCarter and Price 2014). Thus, *S. rubellum* and *S. fuscum* occupy the driest microtopography; however, *S. rubellum* can thrive in a larger range of moisture (Robroek et al 2007; Rydin and Mcdonald 2013). *S. magellanicum* is large and loosely packed in Eastern Canada, resulting in more large pores; thus occupies a wetter microtopographic position (McCarter and Price 2014). As such, it is possible that different pore sizes from each species are overlapping such that the initial drainage of the 2006 profile between 0 to -10 cm of pressure is different from that of 1970 profile.

Retention curves parameterized with the same approach were very similar between both profiles, with the exception of DUAL free $_{dry}$, for previously mentioned reasons (Figure 3-2). The similarity would suggest that there is a similar structure in the moss, which could be due in part to the large proportions of *S.rubellum* in both profiles. Although it does not seem like macroporosity extends to layer 2 of the 2006 profile, the presence of *S. magellanicum* may be responsible for the quicker drainage than the 1970 profile found in all approaches.

The unimodal approaches were unable to represent the bimodal nature of the retention curve during periods near saturation (e.g. hours 0-480 Figure 3-3; Figure 3-2). It is possible that an approach that includes hysteresis and dual porosity would better simulate the 2006 profile (*e.g.* Toride et al 2012). As previously mentioned, *Sphagnum* and peat substrates strongly exhibit hysteretic behaviour; although the specific mechanisms of hysteresis have not been explored, its inclusion is beneficial to simulating soil moisture at the field scale in regenerated peatlands. Furthermore, it is important to prevent the pumping effect by using the implementation of hysteresis proposed by Kool and Parker (1987). Although not explicit in the 1970 profile it is likely pumping occurred in the 2006 profile; simulated soil moisture was uncharacteristically drier than the observed soil moisture in layer 1 (Figure 3-7). HYST no pump $_{dry}$ performed better than HYST pump $_{dry}$ because simulated soil moisture was more accurately predicted after reversal points that were not on the main wetting or drying curves. The parameters from the HYST no pump $_{dry}$ approach were adequate for predicting soil moisture in managed peatlands with similar species composition.

Although a fairly robust parameter set was developed (HYST no pump $_{dry}$) for managed systems, it is unclear how accurate prediction will be during periods of drought when observed soil moisture is far below the calibration period. Schwärzel et al (2006a) has suggested that inverse simulation of parameters using transient laboratory experiments performs similarly to those estimated from transient field experiments. As such, a wider range of soil moisture could be made available for calibration.

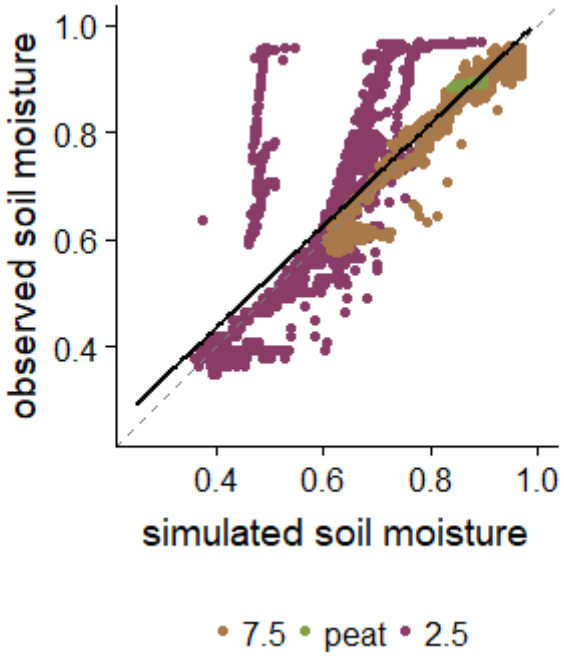

Figure 3-7: Illustration of the pumping effect

Regression of the simulated and observed soil moisture for the HYST pump dry approach in the 2006 profile.

3.5 Conclusion

Inverse simulation of field observations of soil moisture was able to produce acceptable parameter sets for approaches that include hysteresis or dual porosity. Observations of hysteresis in *Sphagnum* and peat have been pervasive throughout the literature, yet this is the first study in which it was included in an unsaturated model. Including hysteresis markedly improved the simulation of soil moisture in regenerated *Sphagnum* moss at the field scale, provided it is an implementation that prevents the pumping effect. The utility of a dual porosity approach was mixed, as the additional parameters increase the likelihood of parameter non-uniqueness compared to the VGM. The advantage, however, is that substrates that do exhibit dual porosity are better represented, which may be related to the mix of moss species. For applications in *Sphagnum* fibre farming it is recommended

that the hysteresis approach be used over the dual porosity approach because hysteresis is a more dominant and universal process.

The validity of the estimated parameters was highly dependent on the observed soil moisture range of the calibration period. The calibration in the dry period estimated parameters that are appropriate for use in managed peatlands, where the water table is maintained close to the surface. In natural peatlands, especially during drought, caution should be used when extrapolating beyond the calibration range. Future work should focus on the parameterization different *Sphagnum* moss species to better represent heterogeneity of unsaturated processes at the field scale.

Chapter 4
Conclusions & Recommendations

The two parameter estimation techniques explored in this study generated parameters that resulted simulations of soil moisture when subject to the same boundary conditions. The study showed that parameters estimated from steady state laboratory (SSL) experiments were unable to simulate soil moisture at a field scale, whereas parameters estimated from transient field (TF) experiments were. The main difference between SSL and TF parameters was that SSL VGM parameter α was several times larger than TF α; which resulted in drainage occurring closer to 0 cm of pressure. It is hypothesized that α was overestimated in the SSL parameterization because drainage may have occurred before the experiment began; thus, parameters represent a scanning curve as opposed to the main drying curve. Further work into explaining why the laboratory retention curves underestimated α is needed. Inverse estimation of parameters from TF experiments is recommended when the objective is to accurately predict field scale unsaturated processes because it better characterizes α, which was found to be the most sensitive parameter.

Despite the satisfactory fit of the VGM, periods of abrupt soil moisture variability (precipitation), and drying beyond the calibration range were not well represented. A dual porosity approach was able to better simulate soil moisture in the wet range (0 to -8 cm of pressure) of the 2006 profile. Dual porosity in the 2006 profile was most likely due to the mix of *Sphagnum* species associated with different microforms. The species composition of a moss profile could have a substantial impact on the retention properties and warrants further study.

Sphagnum moss and peat have been long established as porous media that exhibit a strong degree of hysteresis; representing it in unsaturated models increased performance where other approaches were insufficient. Hysteresis was a better approach because it represents all possible retention curves; whereas the VGM and dual porosity approaches are an aggregate of wetting and drying processes. It is important that implementations of hysteresis are designed to avoid the pumping effect, as it can lead to unrealistic estimations of soil moisture. Including hysteresis may be particularly important for irrigated *Sphagnum* fibre farming operations because water table may fluctuate more than in a natural system to maintain a constant level.

Successful calibration of all approaches was highly dependent of the range of observed soil moisture during the calibration period. The wet calibration had very little variation in soil moisture and the poor calibration was reflected in high model error. The soil moisture range of the dry

calibration was limited compared to what some peatlands can experience; as such it is suggested that parameter estimates from this study could be used to predict the soil moisture response for *Sphagnum* fibre farming. It is unclear if the estimated parameters can be used to predict soil moisture in a natural system where conditions may be drier than the calibration period. A good calibration needs to cover a wide range of soil moisture for both wetting and drying curves. Transient laboratory experiments may be better suited because drying can be controlled, whereas in the field it is limited by atmospheric conditions.

The intended use of models for *Sphagnum* fibre farming are to determine the minimum water table threshold, how the minimum water table may change over time, and estimate the water demand of an operation. It is recommended that parameterization of the desired species is done to characterize the surface and sub-surface layers. Further work should be done to assess how the retention properties change as moss ages to determine how many layers and observation points are needed to accurately represent the moss profile.

References

Bashir R, Sharma J, Stefaniak H (2016) Effect of hysteresis of soil-water characteristic curves on infiltration under different climatic conditions. Canadian Geotechnical Journal 53:273–284. doi: 10.1139/cgj-2015-0004

Benscoter BW, Thompson DK, Canada NR, et al (2011) Interactive effects of vegetation, soil moisture and bulk density on depth of burning of thick organic soils. doi: 10.1071/WF08183

Beven K (1993) Prophecy, reality and uncertainty in distributed hydrological modelling. Advances in Water Resources 16:41–51. doi: 10.1016/0309-1708(93)90028-E

Bloemen GW (1983) Calculation of hydraulic conductivities and steady state capillary rise in peat soils from bulk density and solid matter volume. Zeitschrift für Pflanzenernährung und Bodenkunde 146:460–473. doi: 10.1002/jpln.19831460407

Brown CM, Strack M, Price JS (2017) The effects of water management on the CO 2 uptake of Sphagnum moss in a reclaimed peatland. Mires and Peat 20:1–15. doi: 10.19189/MaP.2016.OMB.258

Carrera J, Neuman SP (1986) Estimation of Aquifer Parameters Under Transient and Steady State Conditions: 2. Uniqueness, Stability, and Solution Algorithms. Water Resources Research 22:211–227.

Clymo RS (1973) The Growth of Sphagnum : Some Effects of Environment. Journal of Ecology 61:849–869. doi: 10.2307/2258654

da Silva FF, Wallach R, Chen Y (1993) Hydraulic properties of sphagnum peat moss and tuff (scoria) and their potential effects on water availability. Plant and Soil 154:119–126. doi: 10.1007/BF00011080

Daniel C, Woods FS (1980) Fitting equations to data: computer analysis of multifactor data. John Wiley & Sons, Inc.

Dettmann U, Bechtold M, Frahm E, Tiemeyer B (2014) On the applicability of unimodal and bimodal van Genuchten-Mualem based models to peat and other organic soils under evaporation conditions. Journal of Hydrology 515:103–115. doi: 10.1016/j.jhydrol.2014.04.047

Diamantopoulos E, Durner W, Reszkowska A, Bachmann J (2013) Effect of soil water repellency on soil hydraulic properties estimated under dynamic conditions. Journal of Hydrology 486:175–

186. doi: 10.1016/j.jhydrol.2013.01.020

Dixon SJ, Kettridge N, Moore PA, et al (2017) Peat depth as a control on moss water availability under evaporative stress. Hydrological Processes 31:4107–4121. doi: 10.1002/hyp.11307

Durner W (1994) Hydraulic conductivity estimation for soils with heterogeneous pore structure. Water Resources Research 30:211–223.

Flanagan TGW-LB (1996) Effect of changes in water content on photosynthesis , transpiration and discrimination against 13C02 and C180160 in Pleurozium and Sphagnum. Oecologia 2:38–46.

Freeman C, Reynolds B (1993) Impacts of climatic change on peatland hydrochemistry; a laboratory-based experiment. 8:49–59.

Gaudig G, Krebs M, Prager A, et al (2018) Sphagnum farming from species selection to the production of growing media : a review. 20:1–30. doi: 10.19189/MaP.2018.OMB.340

Gauthier TLJ, McCarter CPR, Price JS (2018) The effect of compression on Sphagnum hydrophysical properties: Implications for increasing hydrological connectivity in restored cutover peatlands. Ecohydrology 11:1–11. doi: 10.1002/eco.2020

Ghanbarian B, Hunt AG, Ewing RP, Sahimi M (2013) Tortuosity in Porous Media: A Critical Review. Soil Science Society of America Journal 77:1461. doi: 10.2136/sssaj2012.0435

Gharedaghloo B, Price JS (2019) Characterizing the immiscible transport properties of diesel and water in peat soil. Journal of Contaminant Hydrology 221:11–25. doi: 10.1016/j.jconhyd.2018.12.005

Gharedaghloo B, Price JS (2018) Fate and transport of free-phase and dissolved-phase hydrocarbons in peat and peatlands : developing a conceptual model. 68:55–68.

Gharedaghloo B, Price JS, Rezanezhad F, Quinton WL (2018) Evaluating the hydraulic and transport properties of peat soil using pore network modeling and X-ray micro computed tomography. Journal of Hydrology 561:494–508. doi: 10.1016/j.jhydrol.2018.04.007

Gnatowski T, Szatylowicz J, Brandyk T (2002) Effect of peat decomposition on the capillary rise in peat-moorsh soils from the Biebrza River Valley. International Agrophysics 16:97–102.

Gnatowski T, Szatyłowicz J, Brandyk T, Kechavarzi C (2010) Hydraulic properties of fen peat soils in Poland. Geoderma 154:188–195. doi: 10.1016/j.geoderma.2009.02.021

Goetz JD, Price JS (2015) Role of morphological structure and layering of *Sphagnum* and *Tomenthypnum* mosses on moss productivity and evaporation rates. Canadian Journal of Soil Science 95:109–124. doi: 10.4141/cjss-2014-092

Golubev V (2018) The effects of volume change and depth/species type on the hydrophysical properties of Sphagnum moss. Brandon University

Golubev V, Whittington PN (2018) Effects of volume change on the unsaturated hydraulic conductivity of Sphagnum moss. Journal of Hydrology 559:884–894. doi: 10.1016/j.jhydrol.2018.02.083

Hájek T, Beckett RP (2008) Effect of water content components on desiccation and recovery in Sphagnum mosses. Annals of Botany 101:165–173. doi: 10.1093/aob/mcm287

Hallema DW, Périard Y, Lafond JA, et al (2015) Characterization of Water Retention Curves for a Series of Cultivated Histosols. Vadose Zone Journal 14:0. doi: 10.2136/vzj2014.10.0148

Hayward P., Clymo RS (1982) Profiles of Water Content and Pore Size in Sphagnum and Peat , and their Relation to Peat Bog Ecology Author (s): P . M . Hayward and R . S . Clymo Published by : Royal Society Stable URL : http://www.jstor.org/stable/35511 Accessed : 02-03-2016 02 : 00. Proceedings of the Royal Society of London. Series B, Biological Sciences 215:299–325.

Hopmans JW, Šimůnek J, Romana N, Durner W (2002) Inverse Methods. In: Dane JH, Topp GC (eds) Methods of Soil Analysis: Part 4 Physical Methods. SSSA, Madison, WI, pp 963–1008

Kettridge N, Tilak AS, Devito KJ, et al (2016) Moss and peat hydraulic properties are optimized to maximize peatland water use efficiency. Ecohydrology 9:1039–1051. doi: 10.1002/eco.1708

Kling H, Fuchs M, Paulin M (2012) Runoff conditions in the upper Danube basin under an ensemble of climate change scenarios. Journal of Hydrology 424–425:264–277. doi: 10.1016/j.jhydrol.2012.01.011

Konikow LF, Bredehoeft JD (1992) Ground-water models cannot be validated. Advances in Water Resources 15:75–83.

Kool JB, Parker JC (1987) Development and evaluation of closed-form expressions for hysteretic soil hydraulic properties. Water Resources Research 23:105–114. doi: 10.1029/WR023i001p00105

Kool JB, Parker JC, van Genuchten MT (1987) Parameter estimation for unsaturated flow and transport models - A review. Journal of Hydrology 91:255–293. doi: 10.1016/0022-

1694(87)90207-1

Kosugi K, Hopmans JW, Dane JH (2002) Parametric Models. In: Hopmans JANW, Dane JH (eds) Methods of Soil Analysis: Part 4 Physical Methods. SSSA, Madison, WI, pp 728–757

Landry J, Rochefort L (2009) Experimental Sphagnum farming station, Shippagan, New Brunswick: Activity report 2003-2008.

Lewis AM (1988) A test of the air-seeding hypothesis using sphagnum hyalocysts. Plant Physiology 87:577–582. doi: 10.1104/pp.87.3.577

Lindholm T, Markkula I (1984) Moisture conditions in hummocks and hollows in virgin and drained sites on the raised bog Laaviosuo, southern Finland. Annales Botanici Fennici 21:241–255.

Londra PA (2010) Simultaneous determination of water retention curve and unsaturated hydraulic conductivity of substrates using a steady-state laboratory method. HortScience 45:1106–1112.

Mauricio Zambrano-Bigiarini (2017) hydroGOF: Goodness-of-fit functions for comparison of simulated and observed hydrological time series. doi: 10.5281/zenodo.840087

McCarter CPR, Ketcheson SJ, Weber TKD, et al (2017) Modified Technique for Measuring Unsaturated Hydraulic Conductivity in Sphagnum Moss and Peat. Soil Science Society of America Journal 81:747–757. doi: 10.2136/sssaj2007.0111N

McCarter CPR, Price JS (2015) The hydrology of the Bois-des-Bel peatland restoration: Hydrophysical properties limiting connectivity between regenerated Sphagnum and remnant vacuum harvested peat deposit. Ecohydrology 8:173–187. doi: 10.1002/eco.1498

McCarter CPR, Price JS (2014) Ecohydrology of Sphagnum moss hummocks: Mechanisms of capitula water supply and simulated effects of evaporation. Ecohydrology 7:33–44. doi: 10.1002/eco.1313

McNeil P, Waddington JM (2003) Moisture controls on Sphagnum growth and CO2 exchange on a cutover bog. Journal of Applied Ecology 40:354–367. doi: 10.1046/j.1365-2664.2003.00790.x

Mesplé F, Troussellier M, Casellas C, Legendre P (1996) Evaluation of simple statistical criteria to qualify a simulation. Ecological Modelling 88:9–18. doi: 10.1016/0304-3800(95)00033-X

Michel JC, Rivière LM, Bellon-Fontaine MN (2001) Measurement of the wettability of organic materials in relation to water content by the capillary rise method. European Journal of Soil

Science 52:459–467. doi: 10.1046/j.1365-2389.2001.00392.x

Moore PA, Morris PJ, Waddington JM (2015) Multi-decadal water table manipulation alters peatland hydraulic structure and moisture retention. Hydrological Processes 29:2970–2982. doi: 10.1002/hyp.10416

Moore PA, Waddington JM (2015) Modelling Sphagnum moisture stress in response to projected 21 st century climate change. Hydrological Processes 29:3966–3982. doi: 10.1002/hyp.10484

Mualem Y (1976) A New Model for Predicting the Hydraulic Conductivity of Unsaturated Porous Media. Water Resources Research 12:564–566. doi: 10.1029/WR012i003p00564

Naasz R, Michel J-C, Charpentier S (2005) Measuring Hysteretic Hydraulic Properties of Peat and Pine Bark using a Transient Method. Soil Science Society of America Journal 69:13. doi: 10.2136/sssaj2005.0013

Naasz R, Michel JC, Charpentier S (2008) Water repellency of organic growing media related to hysteretic water retention properties. European Journal of Soil Science 59:156–165. doi: 10.1111/j.1365-2389.2007.00966.x

Nash JE, Sutcliffe J V (1970) River Flow Forecasting Through Conceptual Models Part I-a Discussion of Principles*. Journal of Hydrology 10:282–290. doi: 10.1016/0022-1694(70)90255-6

Nijp JJ, Metselaar K, Limpens J, et al (2017) Including hydrological self-regulating processes in peatland models: Effects on peatmoss drought projections. Science of the Total Environment 580:1389–1400. doi: 10.1016/j.scitotenv.2016.12.104

Parker JC, Lenhard RJ (1987) A Model for Hysteric Constitutive Relations Governing Multiphase Flow 1. Saturation-Pressure Relations. Water Resources Research 23:2187–2196.

Paternoster R, Brame R, Mazerolle P, Piquero A (1998) Using the correct statistical test for the equality of regression coefficients. Criminology 36:859–866. doi: 10.1111/j.1745-9125.1998.tb01268.x

Peters A, Durner W, Wessolek G (2011) Consistent parameter constraints for soil hydraulic functions. Advances in Water Resources 34:1352–1365. doi: 10.1016/j.advwatres.2011.07.006

Petrone RM, Devito KJ, Silins U, et al (2008) Transient peat properties in two pond-peatland complexes in the sub-humid Western Boreal Plain , Canada. Mires and Peat 3:1–13.

Piñeiro G, Perelman S, Guerschman JP, Paruelo JM (2008) How to evaluate models: Observed vs. predicted or predicted vs. observed? Ecological Modelling 216:316–322. doi: 10.1016/j.ecolmodel.2008.05.006

Pouliot R, Hugron S, Rochefort L (2015) Sphagnum farming: A long-term study on producing peat moss biomass sustainably. Ecological Engineering 74:135–147. doi: 10.1016/j.ecoleng.2014.10.007

Price JS (1997) HYDROLOGY AND MICROCLIMATE OF A PARTLY RESTORED CUTOVER BOG , QUEBEC. 10:1263–1272.

Price JS (1992) Blanket bog in Newfoundland. Part 2. Hydrological processes. Journal of Hydrology 135:103–119. doi: 10.1016/0022-1694(92)90083-8

Price JS, Whittington PN (2010) Water flow in Sphagnum hummocks: Mesocosm measurements and modelling. Journal of Hydrology 381:333–340. doi: 10.1016/j.jhydrol.2009.12.006

Price JS, Whittington PN, Elrick DE, et al (2008) A Method to Determine Unsaturated Hydraulic Conductivity in Living and Undecomposed Moss. Soil Science Society of America Journal 72:487. doi: 10.2136/sssaj2007.0111N

Priesack E, Durner W (2006) Closed-Form Expression for the Multi-Modal Unsaturated Conductivity Function. Vadose Zone Journal 5:121. doi: 10.2136/vzj2005.0066

Priestley CH., Taylor RJ (1972) On the Assessment of Surface Heat Flux and Evaporation Using Large-Scale Parameters. Monthly Weather Review 100:81–92. doi: 10.1175/1520-0493(1972)100<0081:OTAOSH>2.3.CO;2

Quinton WL, Elliot T, Price JS, et al (2009) Measuring physical and hydraulic properties of peat from X-ray tomography. Geoderma 153:269–277. doi: 10.1016/j.geoderma.2009.08.010

R Core Team (2018) R: A Language and Environment for Statistical Computing.

Rezanezhad F, Price JS, Craig JR (2012) The effects of dual porosity on transport and retardation in peat: A laboratory experiment. Canadian Journal of Soil Science 92:723–732. doi: 10.4141/cjss2011-050

Rezanezhad F, Price JS, Quinton WL, et al (2016) Structure of peat soils and implications for water storage , fl ow and solute transport : A review update for geochemists. Chemical Geology 429:75–84. doi: 10.1016/j.chemgeo.2016.03.010

Rezanezhad F, Quinton WL, Price JS, et al (2010) Influence of pore size and geometry on peat unsaturated hydraulic conductivity computed from 3D computed tomography image analysis. Hydrological Processes 24:2983–2994. doi: 10.1002/hyp.7709

Robroek BJM, Limpens J, Breeuwer A, Schouten MGC (2007) Effects of water level and temperature on performance of four Sphagnum mosses. Plant Ecology 97–107. doi: 10.1007/s11258-006-9193-5

Russo D (1988) Determining Soil Hydraulic Properties by Parameter Estimation- On the Selection of a Model for the Hydraulic Propertie. WATER RESOURCES RESEARC 24:453–459.

Rydin H, Mcdonald AJS (2013) Tolerance of Sphagnum to water level. doi: 10.1179/jbr.1985.13.4.571

Schaap MG, Leij FJ (2000) with the Mualem-van Genuchten Model. 843–851.

Schelle H, Heise L, Jänicke K, Durner W (2013) Water retention characteristics of soils over the whole moisture range: A comparison of laboratory methods. European Journal of Soil Science 64:814–821. doi: 10.1111/ejss.12108

Schwärzel K, Renger M, Sauerbrey R, Wessolek G (2002) Soil physical characteristics of peat soils. Journal of Plant Nutrition and Soil Science 165:479–486. doi: 10.1002/1522-2624(200208)165:4<479::AID-JPLN479>3.0.CO;2-8

Schwärzel K, Šimůnek J, Stoffregen H, et al (2006a) Estimation of the Unsaturated Hydraulic Conductivity of Peat Soils. Vadose Zone Journal 5:628. doi: 10.2136/vzj2005.0061

Schwärzel K, Šimůnek J, Van Genuchten MT, Wessolek G (2006b) Measurement and modeling of soil-water dynamics and evapotranspiration of drained peatland soils. Journal of Plant Nutrition and Soil Science 169:762–774. doi: 10.1002/jpln.200621992

Scott PS, Faraquhar GJ, Kouwen N (1983) Hysteretic Effects on Net Infiltration. Advances in Infiltration. American Society of Agricultural Engineers, Chicago, pp 163–170

Sherwood JH, Kettridge N, Thompson DK, et al (2013) Effect of drainage and wildfire on peat hydrophysical properties. Hydrological Processes 27:1866–1874. doi: 10.1002/hyp.9820

Silvola J (1990) Combined effects of varying water content and CO2 concentration on photosynthesis in Spagnum fuscum. Holartic Ecology 13:224–228.

Simhayov RB, Weber TKD, Price JS (2018) Saturated and unsaturated salt transport in peat from a constructed fen. Soil 4:63–81.

Šimůnek J, Hopmans JW (2002) Parameter Optimization and Nonlinear Fitting. In: Dane JH, Topp CG (eds) Methods of Soil Analysis: Part 4 Physical Methods. SSSA, Madison, WI, pp 139–157

Šimůnek J, Sejna M, Saito H, et al (2009) "The HYDRUS-1D software package for simulating the one-dimensional movement of water, heat, and multiple solutes in variably-saturated media. Version 4.08. HYDRUS Softw. Ser. 3. Dep. of Environ. Sci., Univ. of Calif., Riverside. 332.

Šimůnek J, van Genuchten MT, Šejna M (2012) HYDRUS: Model Use, Calibration, and Validation. Transactions of the ASABE 55:1263–1276. doi: 10.13031/2013.42239

Snowling SD, Kramer JR (2001) Evaluating modelling uncertainty for model selection. Ecological Modelling 138:17–30. doi: 10.1016/S0304-3800(00)00390-2

Strack M, Price JS (2010) Moisture controls on carbon dioxide dynamics of peat-Sphagnum monoliths. Ecohydrology 130:126–130. doi: 10.1002/eco

Sullivan GM, Feinn R (2012) Using Effect Size—or Why the P Value Is Not Enough. Journal of Graduate Medical Education 279–282.

Taylor KE (2001) Summarizing multiple aspects of model performance in a single diagram. Journal of Geophysical Research 106:7183–7192. doi: 10.1007/BF00139495

Taylor N, Price JS (2015) Soil water dynamics and hydrophysical properties of regenerating Sphagnum layers in a cutover peatland. Hydrological Processes 29:3878–3892. doi: 10.1002/hyp.10561

Thompson D, Waddington J (2008) Sphagnum under pressure: towards an ecohydrological approach to examining Sphagnum productivity. Ecohydrology 308:299–308.

Toride N, Sakai M, Šimůnek J (2012) A Hysteretic Model of Hydraulic Properties for Dual-Porosity Soils. Soil Science Society of America Journal 77:1182–1188. doi: 10.2136/sssaj2012.0339n

Tuller M, Or D (2004) Retention of Water in Soil and the Soil Water. In: Hillel D (ed) Encyclopedia of Soils in the Environment, 4th edn. Elsevier Acadmic Press, pp 278–289

van Genuchten MT (1980) A Closed-form Equation for Predicting the Hydraulic Conductivity of Unsaturated Soils1. Soil Science Society of America Journal 44:892. doi:

10.2136/sssaj1980.03615995004400050002x

van Genuchten MT, Leij FJ, Yates SR (1991) The RETC Code for Quantifying the Hydraulic Functions of Unsaturated Soils. United States Environmental Reseach Laboratory 93. doi: 10.1002/9781118616871

Vogel HJ (2000) A numerical experiment on pore size , pore connectivity , water retention , permeability , and solute transport using network models. European Journal of Soil Science 51:99–105.

Vrugt JA, Stauffer PH, Wöhling T, et al (2008) Inverse Modeling of Subsurface Flow and Transport Properties: A Review with New Developments. Vadose Zone Journal 7:843. doi: 10.2136/vzj2007.0078

Wallor E, Herrmann A, Zeitz J (2018) Hydraulic properties of drained and cultivated fen soils part II — Model-based evaluation of generated van Genuchten parameters using experimental field data. Geoderma 319:208–218. doi: 10.1016/j.geoderma.2017.12.012

Weber TKD, Iden SC, Durner W (2017a) Unsaturated hydraulic properties of Sphagnum moss and peat reveal trimodal pore-size distributions. Water Resources Research 415–434. doi: 10.1002/2016WR019707.Received

Weber TKD, Iden SC, Durner W (2017b) A pore-size classification for peat bogs derived from unsaturated hydraulic properties. Hydrology and Earth System Sciences 21:6185–6200. doi: 10.5194/hess-21-6185-2017

Weiss R, Alm J, Laiho R, Laine J (1998) Modeling Moisture Retention in Peat Soils. Soil Science Society of America Journal 62:305. doi: 10.2136/sssaj1998.03615995006200020002x

Wösten JHM, Van Genuchten MT (1988) Using texture and other soil properties to predict the unsaturated soil hydraulic functions. Soil Science Society of America Journal 6:1762–1770. doi: 10.1201/9781351073073

Zhang Z, Thiery M, Baroghel-bouny V (2014) A review and statistical study of existing hysteresis models for cementitious materials. Cement and Concrete Research 57:44–60.

Appendix A

Compilation of Literature VGM Parameters

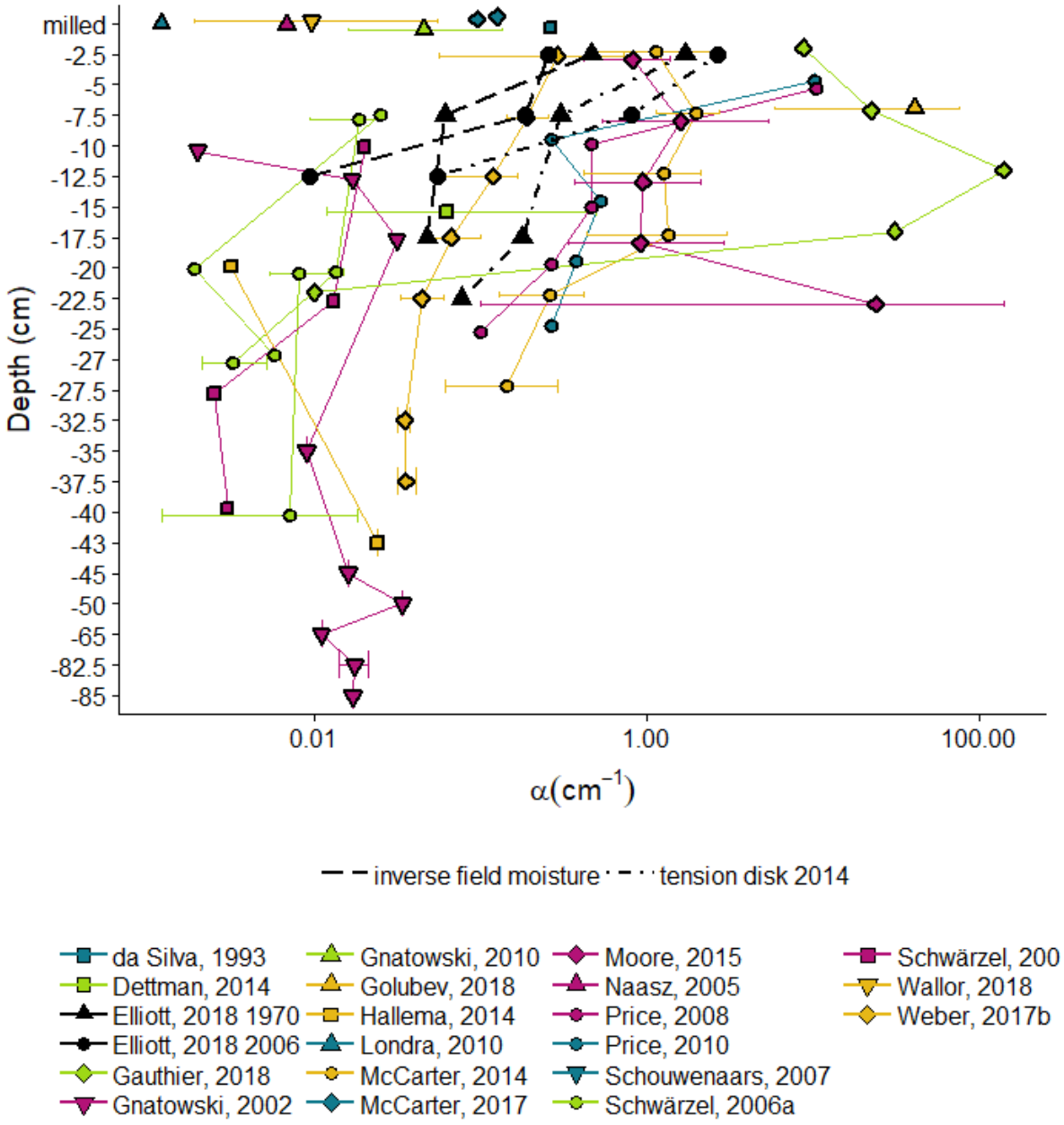

Figure A-1: combination plot of all literature values for α.

Points are the average value, and the error bars are the maximum and minimum values reported.

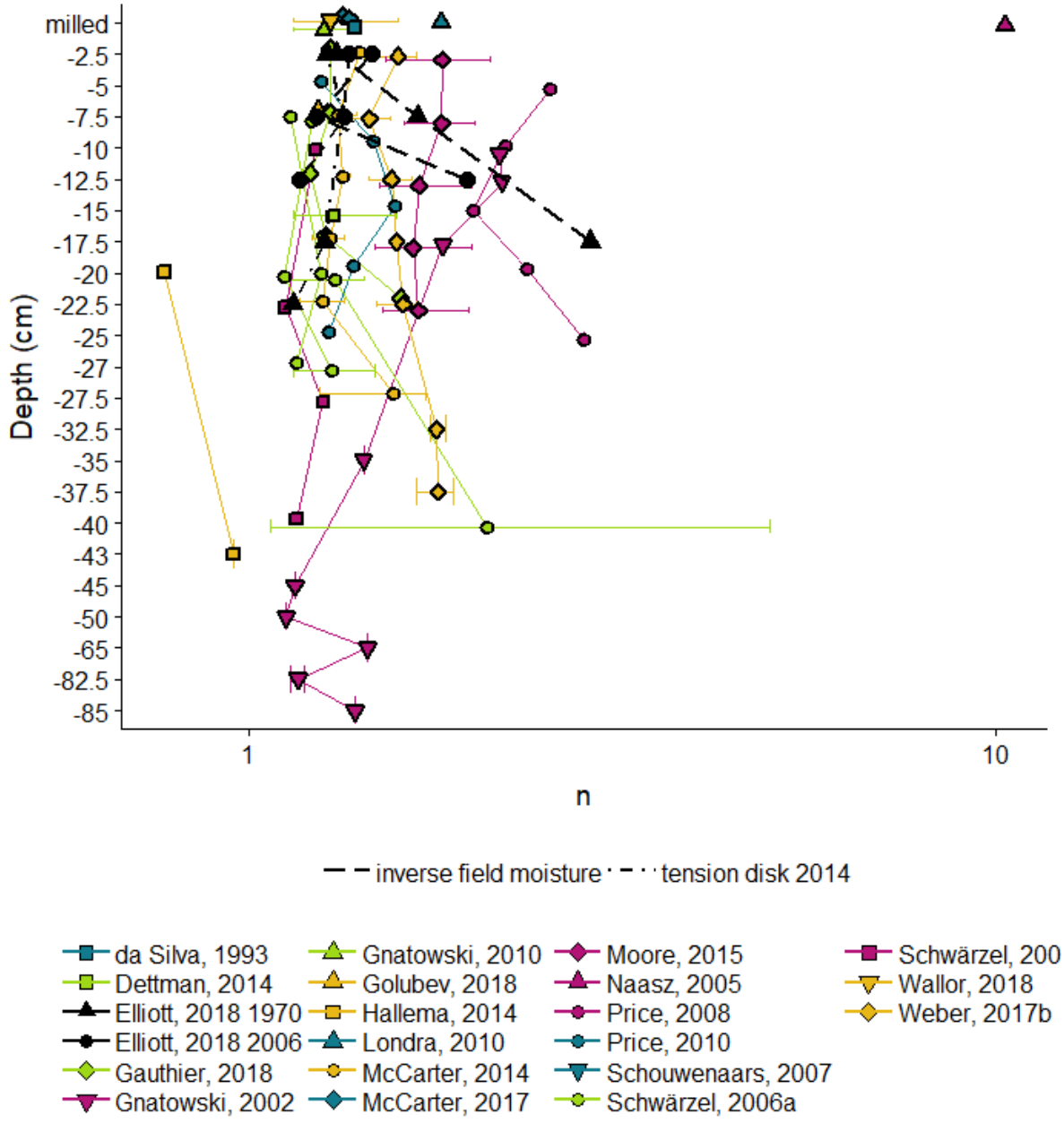

Figure A-4-2: combination plot of all literature values for n.

Points are the average value, and the error bars are the maximum and minimum values reported.

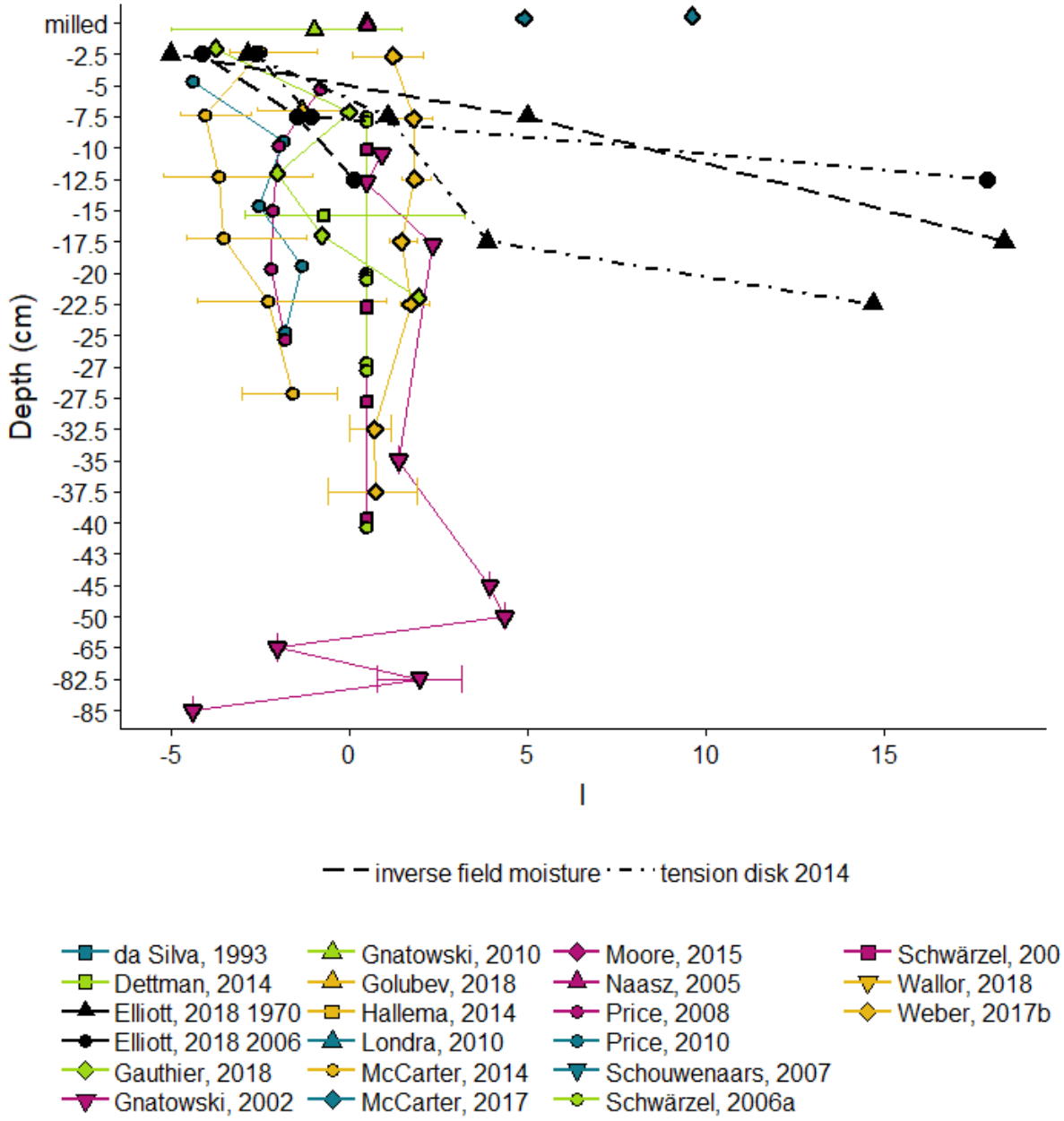

Figure A-3: combination plot of all literature values for I.

Points are the average value, and the error bars are the maximum and minimum values reported.

Appendix B

Initial Parameter Estimates for Chapter 2

Table B-1: Initial parameter estimates for curve fitting in RETC and inverse modeling in Hydrus-1D

Method	Plot	Depth	θr	θs	α (cm^{-1})	n	K_s ($cm\ d^{-1}$)	l
SSL	1970	2.5	0.11	0.97	0.5	1.56	4699	0.5
SSL	1970	7.5	0.11	0.95	0.04	1.56	6959	0.5
SL	1970	17.	0.05	0.94	0.04	1.56	3703	0.5
SSL	1970	peat	0.05	0.94	0.04	1.56	913	20
SSL	2006	2.5	0.11	0.98	2	1.56	9397	0.5
SSL	2006	7.5	0.11	0.97	20	1.1	7310	-6
SSL	2006	peat	0.05	0.93	0.04	1.56	910	0.5
TF	1970	2.5	0.11	0.97	1.71	1.28	4699	-2.85
TF	1970	7.5	0.11	0.95	0.3	1.34	6959	1.1
TF	1970	12.5	0.05	0.94	0.18	1.27	3703	3.87
TF	1970	peat	0.05	0.9	0.01	1.96	912	0.16
TF	2006	2.5	0.11	0.98	2.7	1.37	9397	-2.61
TF	2006	7.5	0.11	0.97	1.5	1.34	7310	-1.08
TF	2006	peat	0.05	0.9	0.01	1.17	909	17.92
ALT	1970	2.5	0.11	0.97	0.29	1.6	4699	1.24
ALT	1970	7.5	0.11	0.95	0.19	1.45	6959	1.82
ALT	1970	12.5	0.05	0.94	0.09	1.57	3703	1.65
ALT	1970	peat	0.05	0.9	0.01	1.21	912	1.87
ALT	2006	2.5	0.11	0.98	0.29	1.59	9397	1.24
ALT	2006	7.5	0.11	0.97	0.19	1.45	7310	1.82
ALT	2006	peat	0.05	0.9	0.01	1.17	909	17.92

Appendix C

Initial Parameter Estimates for Chapter 2

Table C-1: Initial parameter estimates for inverse estimation of parameter in Hydrus-1D for the VGM approach.

Plot	Approach	θr	θs	α (cm^{-1})	n	K_s ($cm\ d^{-1}$)	l
1970	VGM_{dry}	0.11	0.97	1.71	1.28	4699	-2.85
1970	VGM_{dry}	0.11	0.95	0.3	1.34	6959	1.1
1970	VGM_{dry}	0.05	0.94	0.18	1.27	3703	3.87
1970	VGM_{dry}	0.05	0.9	0.01	1.96	912	0.16
1970	VGM_{wet}	0.11	0.97	0.5	1.28	4699	-2.85
1970	VGM_{wet}	0.11	0.97	0.3	1.34	6959	1.1
1970	VGM_{wet}	0.05	0.94	0.18	1.27	3703	3.87
1970	VGM_{wet}	0.05	0.9	0.01	1.96	912	0.16
2006	VGM_{dry}	0.11	0.98	2.7	1.37	9397	-2.61
2006	VGM_{dry}	0.11	0.97	1.5	1.34	7310	-1.08
2006	VGM_{dry}	0.05	0.9	0.01	1.17	909	17.92
2006	VGM_{wet}	0.11	0.98	0.13	1.3	9397	-2.61
2006	VGM_{wet}	0.11	0.97	0.1	1.4	7310	-1.08
2006	VGM_{wet}	0.05	0.9	0.01	1.01	909	17.92

Table C-2: Initial parameter estimates for inverse estimation of parameter in Hydrus-1D for the hysteresis approaches.

Plot	Approach	θr	θs	α (cm^{-1})	n	K_s (cm d^{-1})	l	α_W (cm^{-1})
1970	HYST no pump $_{dry}$	0.11	0.97	0.5	1.28	4699	-2.85	1.71
1970	HYST no pump $_{dry}$	0.11	0.95	0.15	1.34	6959	1.1	0.3
1970	HYST no pump $_{dry}$	0.05	0.94	0.08	1.27	3703	3.87	0.18
1970	HYST no pump $_{dry}$	0.05	0.9	0.01	2	912	17.92	9.48
1970	HYST pump $_{dry}$	0.11	0.97	0.5	1.28	4699	-2.85	1.71
1970	HYST pump $_{dry}$	0.11	0.95	0.15	1.34	6959	1.1	0.3
1970	HYST pump $_{dry}$	0.05	0.94	0.08	1.27	3703	3.87	0.18
1970	HYST pump $_{dry}$	0.05	0.9	0.01	2	912	17.92	9.48
1970	HYST no pump $_{wet}$	0.11	0.97	0.1	1.83	4699	-2.85	0.6
1970	HYST no pump $_{wet}$	0.11	0.975	0.05	1.5	6959	1.1	0.22
1970	HYST no pump $_{wet}$	0.05	0.94	0.05	1.5	3703	3.87	0.02
1970	HYST no pump $_{wet}$	0.05	0.9	0.01	1.96	912	0.16	0.01
2006	HYST no pump $_{dry}$	0.11	0.98	0.25	1.37	9397	-2.61	2.7
2006	HYST no pump $_{dry}$	0.11	0.97	0.25	1.34	7310	-1.08	1.5
2006	HYST no pump $_{dry}$	0.05	0.9	0.01	1.17	909	17.92	0.01
2006	HYST pump $_{dry}$	0.11	0.98	0.25	1.37	9397	-2.61	2.7
2006	HYST pump $_{dry}$	0.11	0.97	0.2	1.34	7310	-1.08	1.5
2006	HYST pump $_{dry}$	0.05	0.9	0.01	1.17	909	17.92	0.1
2006	HYST no pump $_{wet}$	0.11	0.98	0.1	1.87	9397	-2.61	0.34
2006	HYST no pump $_{wet}$	0.11	0.97	0.13	1.29	7310	-1.08	0.43
2006	HYST no pump $_{wet}$	0.05	0.9	0.01	2	909	17.92	9.48

Table C-3: Initial parameter estimates for inverse estimation of parameter in Hydrus-1D for the dual porosity approaches.

Plot	Approach	θr	θs	α (cm^{-1})	n	K_s ($cm\ d^{-1}$)	l	w_2	α_2 (cm^{-1})	n_2
1970	DUAL free $_{dry}$	0.11	0.97	0.5	3	4699	-2.85	0.5	0.03	1.5
1970	DUAL free $_{dry}$	0.11	0.95	0.15	3	6959	1.1	0.5	0.03	1.5
1970	DUAL free $_{dry}$	0.05	0.94	0.08	1.27	3703	3.87	0.5	0.03	1.5
1970	DUAL free $_{dry}$	0.05	0.9	0.04	3	912	17.92	0.81	0.002	1.004
1970	DUAL fix $_{dry}$	0.11	0.97	0.55	2.36	4699	-2.85	0.62	0.04	5
1970	DUAL fix $_{dry}$	0.11	0.95	0.33	2.04	6959	1.1	0.48	0.04	5
1970	DUAL fix $_{dry}$	0.05	0.94	0.36	2.08	3703	3.87	0.47	0.04	5
1970	DUAL fix $_{dry}$	0.05	0.9	0.05	1.87	909	0.16	0.79	0.0002	1.03
1970	DUAL free $_{wet}$	0.11	0.97	0.49	3	4699	-2.85	0.37	0.03	3.11
1970	DUAL free $_{wet}$	0.11	0.975	0.1	3	6959	1.1	0.55	0.04	5.82
1970	DUAL free $_{wet}$	0.05	0.94	0	3	3703	3.87	0.32	0.08	3.68
1970	DUAL free $_{wet}$	0.05	0.9	0.04	3	912	17.92	0.81	0.00002	1.004
2006	DUAL free $_{dry}$	0.11	0.98	0.25	3	9397	-2.61	0.5	0.03	1.5
2006	DUAL free $_{dry}$	0.11	0.97	0.25	3	7310	-1.08	0.5	0.03	1.5
2006	DUAL free $_{dry}$	0.05	0.9	0.01	1.17	909	17.92	0.5	0.03	1.5
2006	DUAL fix $_{dry}$	0.11	0.98	0.55	2.36	9397	-2.61	0.62	0.04	5
2006	DUAL fix $_{dry}$	0.11	0.97	0.33	2.04	7310	-1.08	0.48	0.04	5
2006	DUAL fix $_{dry}$	0.05	0.9	0.03	3	909	17.92	0.5	0.03	1.5
2006	DUAL free $_{wet}$	0.11	0.98	0.29	1.58	9397	-4.11	0.27	0.06	1.57
2006	DUAL free $_{wet}$	0.11	0.97	0.27	1.35	7310	-1.46	0.49	0.03	1.56
2006	DUAL free $_{wet}$	0.05	0.9	0.04	3	909	0.16	0.81	0.002	1.004

Appendix D

Correlation Matrices for approach parameterization in Chapter 3

Table D-1: Correlation matrices for inverse simulation of all approaches

1970 DUAL free $_{dry}$

	α - 2.5	n - 2.5	w2 - 2.5	α2 - 2.5	n2 - 2.5	α - 7.5	n - 7.5	w2 - 7.5	α2 - 7.5	n2 - 7.5	α - 12.5	n - 12.5	w2 - 12.5	α2 - 12.5	n2 - 12.5
α - 2.5	1														
n - 2.5	-0.81	1													
w2 - 2.5	-0.71	0.99	1												
α2 - 2.5	-0.59	0.95	0.98	1											
n2 - 2.5	0.49	-0.89	-0.95	-0.99	1										
α - 7.5	0.03	-0.04	-0.04	-0.04	0.04	1									
n - 7.5	0	0	0	0	0	0.96	1								
w2 - 7.5	0.01	-0.01	-0.01	-0.01	0.01	0.98	0.99	1							
α2 - 7.5	0.01	-0.02	-0.02	-0.01	0.02	0.98	0.99	1	1						
n2 - 7.5	0.07	-0.08	-0.08	-0.07	0.07	-0.61	-0.81	-0.76	-0.75	1					
α - 12.5	0	0.01	0.01	0.01	-0.01	-0.02	-0.01	-0.01	-0.02	0	1				
n - 12.5	0.04	-0.03	-0.03	-0.03	0.02	-0.03	-0.01	-0.01	-0.01	-0.03	0.93	1			
w2 - 12.5	0.02	-0.02	-0.02	-0.01	0.01	-0.03	-0.01	-0.01	-0.01	-0.03	0.98	0.97	1		
α2 - 12.5	-0.1	0.1	0.09	0.08	-0.08	0.04	0	0.01	0.01	0.09	-0.77	-0.88	-0.87	1	
n2 - 12.5	0.15	-0.15	-0.14	-0.13	0.12	-0.04	0.01	0	0	-0.13	0.32	0.57	0.49	-0.84	1

1970 DUAL fix $_{dry}$

	w2 - 2.5	α2 - 2.5	n2 - 2.5	w2 - 7.5	α2 - 7.5	n2 - 7.5	w2 - 12.5	α2 - 12.5	n2 - 12.5
w2 - 2.5	1								
α2 - 2.5	0.98	1							
n2 - 2.5	-0.91	-0.95	1						
w2 - 7.5	0	0	0	1					
α2 - 7.5	0	0	0	0.99	1				
n2 - 7.5	0	0	0	-0.96	-0.98	1			
w2 - 12.5	0	0	0	0	0	0	1		
α2 - 12.5	0	0	0	0	0	0	0.35	1	
n2 - 12.5	0	0	0	0	0	0	-0.9	0.03	1

1970 DUAL free

wet

	α - 2.5	n - 2.5	w2 - 2.5	α2 - 2.5	n2 - 2.5	α - 7.5	n - 7.5	w2 - 7.5	α2 - 7.5	n2 - 7.5	α - 12.5	n - 12.5	w2 - 12.5	α2 - 12.5	n2 - 12.5
α - 2.5	1														
n - 2.5	0.7	1													
w2 - 2.5	0.79	0.98	1												
α2 - 2.5	-0.79	-0.22	-0.4	1											
n2 - 2.5	0.87	0.85	0.94	-0.67	1										
α - 7.5	0.06	0.08	0.07	0	0.05	1									
n - 7.5	0.11	0.11	0.11	-0.04	0.1	0.95	1								
w2 - 7.5	0.47	0.46	0.49	-0.29	0.49	0.7	0.64	1							
α2 - 7.5	-0.48	-0.48	-0.5	0.3	-0.5	-0.66	-0.59	-0.99	1						
n2 - 7.5	-0.39	-0.38	-0.41	0.25	-0.41	-0.37	-0.29	-0.7	0.77	1					
α - 12.5	-0.03	-0.02	-0.04	0.07	-0.06	0.7	0.54	0.8	-0.81	-0.62	1				
n - 12.5	0.03	0.01	0.01	-0.04	0.02	-0.41	-0.46	-0.01	-0.03	-0.13	0.06	1			
w2 - 12.5	0.01	0.01	0	0.03	-0.01	0.52	0.33	0.7	-0.72	-0.59	0.9	0.45	1		
α2 - 12.5	0	0	0.01	-0.03	0.02	-0.47	-0.34	-0.71	0.72	0.58	-0.87	-0.39	-0.88	1	
n2 - 12.5	0.04	-0.03	-0.01	-0.06	0.01	0.3	0.54	0.22	-0.19	-0.08	0.06	0.08	0.05	-0.15	1

1970 HYST no pump dry

	α - 2.5	n - 2.5	l - 2.5	αw - 2.5	α - 7.5	n - 7.5	l - 7.5	αw - 7.5	α - 12.5	n - 12.5	l - 12.5	αw - 12.5
α - 2.5	1											
n - 2.5	-1	1										
l - 2.5	0	0	0									
αw - 2.5	0.01	-0.07	0	1								
α - 7.5	0	0	0	0	1							
n - 7.5	0	0	0	0	-0.67	1						
l - 7.5	0	0	0	0	0	0	0					
αw - 7.5	0	0	0	-0.01	-0.13	-0.02	0	1				
α - 12.5	0	0	0	0	0	0	0	0	1			
n - 12.5	0	0	0	0	0	0	0	0	0.92	1		
l - 12.5	0	0	0	0	0	0	0	0	0	0	0	
αw - 12.5	0	0	0	0	0	0	0	0	0	0	0	0

1970 HYST pump dry

	α - 2.5	n - 2.5	l - 2.5	αw - 2.5	α - 7.5	n - 7.5	l - 7.5	αw - 7.5	α - 12.5	n - 12.5	l - 12.5	αw - 12.5
α - 2.5	1											
n - 2.5	-0.74	1										
l - 2.5	0.03	-0.43	1									
αw - 2.5	0.1	-0.01	-0.06	1								
α - 7.5	0.05	-0.47	0.97	-0.02	1							
n - 7.5	0.04	0.14	0.02	-0.18	-0.2	1						
l - 7.5	-0.44	0.05	0.1	0.23	0.1	-0.09	1					
αw - 7.5	0.07	0.02	-0.08	-0.4	-0.13	0.44	-0.11	1				
α - 12.5	0.15	-0.37	0.12	-0.11	0.21	-0.28	0.1	0.05	1			
n - 12.5	-0.02	0.13	-0.02	0.03	-0.1	0.26	-0.09	-0.02	-0.51	1		
l - 12.5	0.09	-0.11	0	0.44	0.12	-0.59	0.01	-0.78	-0.2	0.15	1	
αw - 12.5	-0.21	0.19	0.1	-0.65	0.05	0.16	-0.17	0.19	-0.5	-0.09	-0.15	1

HYST no pump wet

	α - 2.5	n - 2.5	l - 2.5	αw - 2.5	α - 7.5	n - 7.5	l - 7.5	αw - 7.5	α - 12.5	n - 12.5	l - 12.5	αw - 12.5
α - 2.5	1											
n - 2.5	-0.74	1										
l - 2.5	0.03	-0.43	1									
αw - 2.5	0.1	-0.01	-0.06	1								
α - 7.5	0.05	-0.47	0.97	-0.02	1							
n - 7.5	0.04	0.14	0.02	-0.18	-0.2	1						
l - 7.5	-0.44	0.05	0.1	0.23	0.1	-0.09	1					
αw - 7.5	0.07	0.02	-0.08	-0.4	-0.13	0.44	-0.11	1				
α - 12.5	0.15	-0.37	0.12	-0.11	0.21	-0.28	0.1	0.05	1			
n - 12.5	-0.02	0.13	-0.02	0.03	-0.1	0.26	-0.09	-0.02	-0.51	1		
l - 12.5	0.09	-0.11	0	0.44	0.12	-0.59	0.01	-0.78	-0.2	0.15	1	
αw - 12.5	-0.21	0.19	0.1	-0.65	0.05	0.16	-0.17	0.19	-0.5	-0.09	-0.15	1

1970 HYST no pump $_{wet}$

	α - 2.5	n - 2.5	l - 2.5	αw - 2.5	α - 7.5	n - 7.5	l - 7.5	αw - 7.5	α - 12.5	n - 12.5	l - 12.5	αw - 12.5
α - 2.5	1											
n - 2.5	-0.85	1										
l - 2.5	0	0	0									
αw - 2.5	-0.38	0.18	0	1								
α - 7.5	-0.01	-0.01	0	0.02	1							
n - 7.5	0.02	0.01	0	-0.03	-0.68	1						
l - 7.5	0	0	0	0	0	0	0					
αw - 7.5	0	0	0	0	0	0	0	0				
α - 12.5	-0.15	0.26	0	0.21	-0.02	0.02	0	0	1			
n - 12.5	0.09	-0.19	0	-0.16	0.06	-0.09	0	0	-0.99	1		
l - 12.5	0	0	0	0	0	0	0	0	0	0	0	
αw - 12.5	0	0	0	0	0	0	0	0	0	0	0	0

1970 VGM $_{dry}$

	α - 2.5	n - 2.5	l - 2.5	α - 7.5	n - 7.5	l - 7.5	α - 12.5	n - 12.5	l - 12.5
α - 2.5	1								
n - 2.5	-0.99	1							
l - 2.5	-0.06	0.07	1						
α - 7.5	0	0	0	1					
n - 7.5	-0.01	0.01	0.01	-0.91	1				
l - 7.5	0.09	-0.11	-0.84	-0.04	0.05	1			
α - 12.5	0.01	-0.01	-0.1	-0.02	0.04	0.15	1		
n - 12.5	0	-0.01	-0.07	-0.02	0.03	0.1	0.92	1	
l - 12.5	-0.03	0.04	0.51	0.11	-0.2	-0.73	-0.21	-0.14	1

1970 VGM $_{wet}$

	α - 2.5	n - 2.5	l - 2.5	α - 7.5	n - 7.5	l - 7.5	α - 12.5	n - 12.5	l - 12.5
α - 2.5	1								
n - 2.5	-0.94	1							
l - 2.5	-0.01	0	1						
α - 7.5	-0.04	0.03	0.67	1					
n - 7.5	-0.04	0.03	0.69	0.96	1				
l - 7.5	0.04	-0.06	-0.18	-0.06	-0.06	1			
α - 12.5	-0.05	0.07	0.15	-0.08	-0.08	0.27	1		
n - 12.5	0.06	-0.09	-0.21	-0.06	-0.06	-0.26	-0.98	1	
l - 12.5	-0.01	-0.01	0.26	0.55	0.55	-0.3	-0.73	0.57	1

2006 dual free dry

	α - 2.5	n - 2.5	w2 - 2.5	α2 - 2.5	n2 - 2.5	α - 7.5	n - 7.5	w2 - 7.5	α2 - 7.5	n2 - 7.5	α - peat	n - peat	w2 - peat	α2 - peat	n2 - peat
α - 2.5	1														
n - 2.5	0.61	1													
w2 - 2.5	0.77	0.96	1												
α2 - 2.5	0.81	0.92	0.99	1											
n2 - 2.5	-0.81	-0.86	-0.96	-0.99	1										
α - 7.5	-0.03	-0.04	-0.06	-0.06	0.07	1									
n - 7.5	-0.02	-0.03	-0.04	-0.04	0.05	0.98	1								
w2 - 7.5	-0.01	-0.03	-0.03	-0.04	0.04	0.99	0.98	1							
α2 - 7.5	0.01	-0.01	-0.01	-0.01	0.01	0.95	0.93	0.98	1						
n2 - 7.5	-0.03	-0.01	-0.02	-0.02	0.03	-0.89	-0.88	-0.94	-0.99	1					
α - peat	0	0	0.01	0.02	-0.03	0.01	0.02	0.03	0.04	-0.06	1				
n - peat	-0.02	-0.03	-0.02	-0.02	0	0.03	0.03	0.03	0.05	-0.06	0.95	1			
w2 - peat	-0.04	-0.04	-0.04	-0.04	0.02	-0.01	-0.01	-0.01	0	-0.01	0.99	0.98	1		
α2 - peat	-0.21	-0.18	-0.23	-0.25	0.27	-0.26	-0.27	-0.31	-0.36	0.4	0.55	0.64	0.67	1	
n2 - peat	-0.2	-0.17	-0.22	-0.23	0.25	-0.11	-0.12	-0.14	-0.18	0.2	0.76	0.8	0.85	0.94	1

2006 DUAL fix dry

	w2 - 2.5	α2 - 2.5	n2 - 2.5	w2 - 7.5	α2 - 7.5	n2 - 7.5	w2 - peat	α2 - peat	n2 - peat
w2 - 2.5	1								
α2 - 2.5	0.97	1							
n2 - 2.5	-0.9	-0.95	1						
w2 - 7.5	0	0	0	1					
α2 - 7.5	-0.01	-0.01	0.01	-0.43	1				
n2 - 7.5	0	0	0.01	-0.72	0.9	1			
w2 - peat	-0.01	-0.01	0.01	-0.01	0.03	0.02	1		
α2 - peat	0.02	0.02	-0.04	0.02	-0.07	-0.03	0.66	1	
n2 - peat	-0.03	-0.02	0.04	-0.03	0.09	0.05	0.76	0.24	1

2006 DUAL free $_{wet}$

	α - 2.5	n - 2.5	w2 - 2.5	α2 - 2.5	n2 - 2.5	α - 7.5	n - 7.5	w2 - 7.5	α2 - 7.5	n2 - 7.5	α - peat	n - peat	w2 - peat	α2 - peat	n2 - peat
α - 2.5	1														
n - 2.5	-0.91	1													
w2 - 2.5	0.95	-0.75	1												
α2 - 2.5	-0.61	0.21	-0.8	1											
n2 - 2.5	-0.92	0.71	-0.99	0.79	1										
α - 7.5	-0.06	0	-0.09	0.15	0.07	1									
n - 7.5	-0.06	0	-0.09	0.15	0.08	0.92	1								
w2 - 7.5	-0.06	0	-0.09	0.15	0.08	0.99	0.96	1							
α2 - 7.5	0.09	-0.04	0.1	-0.11	-0.09	-0.32	-0.4	-0.35	1						
n2 - 7.5	0.07	-0.01	0.09	-0.13	-0.08	-0.93	-0.78	-0.9	0.45	1					
α - peat	0.05	-0.04	0.05	-0.03	-0.05	0.18	0.18	0.18	0.28	-0.07	1				
n - peat	-0.01	0.04	0.01	-0.07	0	-0.07	-0.06	-0.07	-0.33	-0.01	-0.88	1			
w2 - peat	0.02	-0.01	0.03	-0.03	-0.03	0.07	0.05	0.06	-0.08	-0.09	-0.06	0.29	1		
α2 - peat	0.04	0	0.06	-0.1	-0.05	-0.05	-0.04	-0.04	0	0.03	-0.07	0.03	-0.16	1	
n2 - peat	0	0	0	0	0	0	0	0	0	0	0	0	0	0	0

2006 HYST no pump $_{dry}$

	α - 2.5	n - 2.5	l - 2.5	αw - 2.5	α - 7.5	n - 7.5	l - 7.5	αw - 7.5	α - peat	n - peat	l - peat	αw - peat
α - 2.5	1											
n - 2.5	-0.98	1										
l - 2.5	0	0	0									
αw - 2.5	-0.38	0.23	0	1								
α - 7.5	-0.01	-0.02	0	0.04	1							
n - 7.5	0.02	0.02	0	-0.04	-0.98	1						
l - 7.5	0	0	0	0	0	0	0					
αw - 7.5	-0.15	0.15	0	-0.01	0.05	-0.13	0	1				
α - peat	-0.24	0.26	0	0.13	-0.07	0.08	0	0.11	1			
n - peat	-0.26	0.28	0	0.12	-0.07	0.07	0	0.12	0.64	1		
l - peat	0	0	0	0	0	0	0	0	0	0	0	
αw - peat	-0.08	0.08	0	-0.08	0	0	0	-0.01	-0.13	0.1	0	1

2006 HYST pump wet

	α - 2.5	n - 2.5	l - 2.5	αw - 2.5	α - 7.5	n - 7.5	l - 7.5	αw - 7.5	α - peat	n - peat	l - peat	αw - peat
α - 2.5	1											
n - 2.5	-0.69	1										
l - 2.5	0.6	-0.35	1									
αw - 2.5	0.16	-0.73	-0.02	1								
α - 7.5	0.53	-0.61	0.45	0.29	1							
n - 7.5	-0.38	0.6	-0.21	-0.38	-0.62	1						
l - 7.5	0.11	-0.19	-0.11	0.13	-0.35	0.33	1					
αw - 7.5	0.12	-0.29	-0.03	0.22	-0.02	-0.07	0.37	1				
α - peat	0.05	0.04	0.03	-0.1	0.18	-0.42	-0.43	-0.4	1			
n - peat	0.24	-0.19	0.07	0.02	0.26	-0.11	0.12	-0.1	0.18	1		
l - peat	-0.57	0.64	-0.44	-0.29	-0.96	0.58	0.25	-0.07	-0.14	-0.24	1	
αw - peat	-0.07	0.01	0.04	0.06	-0.12	0.28	0.21	0.16	-0.61	-0.62	0.07	1

2006 HYST no pump wet

	α - 2.5	n - 2.5	l - 2.5	αw - 2.5	α - 7.5	n - 7.5	l - 7.5	αw - 7.5
α - 2.5	1							
n - 2.5	-0.17	1						
l - 2.5	0	0	0					
αw - 2.5	-0.57	-0.03	0	1				
α - 7.5	-0.05	0.15	0	0.22	1			
n - 7.5	0.05	-0.16	0	-0.24	-0.96	1		
l - 7.5	0	0	0	0	0	0	0	
αw - 7.5	-0.03	0.13	0	0.09	0.11	-0.23	0	1

VGM dry

	α - 2.5	n - 2.5	l - 2.5	α - 7.5	n - 7.5	l - 7.5	α - peat	n - peat	l - peat
α - 2.5	1								
n - 2.5	-0.98	1							
l - 2.5	-0.03	0.06	1						
α - 7.5	0.01	-0.02	-0.16	1					
n - 7.5	-0.02	0.02	0.22	-0.98	1				
l - 7.5	0.1	-0.13	-0.93	0.08	-0.14	1			
α - peat	0.01	-0.01	-0.03	-0.01	0.01	0.09	1		
n - peat	0.01	-0.01	-0.03	-0.01	0.01	0.09	0.98	1	
l - peat	-0.01	0.01	-0.03	0.04	-0.03	-0.01	0	0	1

VGM wet

	α - 2.5	n - 2.5	l - 2.5	α - 7.5	n - 7.5	l - 7.5	α - peat	n - peat	l - peat
α - 2.5	1								
n - 2.5	0.08	1							
l - 2.5	-0.04	-0.04	1						
α - 7.5	-0.2	-0.35	0.06	1					
n - 7.5	0.24	0.44	-0.06	-0.96	1				
l - 7.5	-0.25	-0.31	0.27	0.09	-0.14	1			
α - peat	-0.24	-0.29	0.28	0.06	-0.12	0.98	1		
n - peat	-0.05	-0.07	-0.01	-0.09	0.03	0.82	0.84	1	
l - peat	-0.02	0.05	0.53	0.16	-0.14	0.09	0.1	-0.07	1

Appendix E

Regression of Simulated vs. Observed Soil Moisture for Chapter 3

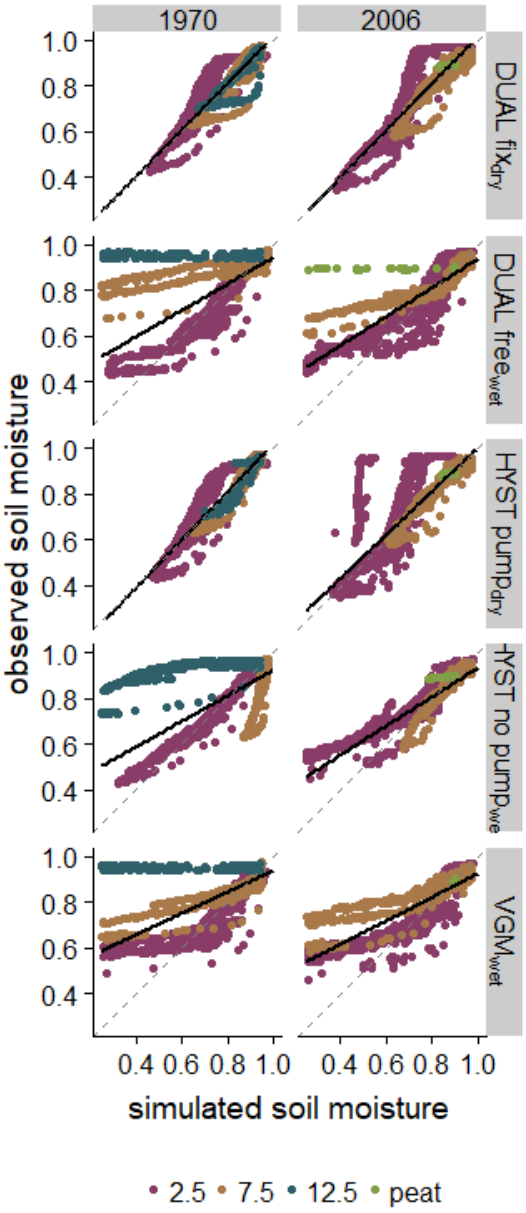

Figure E-1: Regression of the simulated and observed soil moisture for models not included in Figure 6.